Maximum likelihood fitting of single channel NMDA activity with a mechanism composed of independent dimers of subunits

Stephanie Schorge, Sergio Elenes and David Colquhoun

Department of Pharmacology, UCL, London WC1E 6BT, UK

Steady-state single channel activity from NMDA receptors was recorded at a range of concentrations of both glutamate and glycine. The results were fitted with several plausible mechanisms that describe both binding and gating. The mechanisms we have tested were based on our present understanding of receptor structure, or based on previously proposed mechanisms for these receptors. The steady-state channel properties appear to have virtually no dependence on the concentration of either ligand, other than the frequency of channel activations. This limited the ability to discriminate detail in the mechanism, and, along with the persistence of open–shut correlations in high agonist concentrations, suggests that NMDA channels, unlike other neurotransmitter receptors, cannot open unless all binding sites are occupied. As usual for analyses of NMDA channels, the applicability of our results to physiological observations is limited by uncertainties in synaptic zinc and hydrogen ion concentrations, both of these being known to affect the receptor. The mechanism that we propose, on the basis of steady-state single channel recordings, predicts with fair accuracy the apparent open and shut-time distributions in different concentrations of agonists, correlations between open and shut times, and both the rising and falling phases of the macroscopic response to concentration jumps, and can therefore account for the main features of synaptic currents.

(Received 26 July 2005; accepted after revision 23 September 2005; first published online 13 October 2005)
Corresponding author D. Colquhoun: Department of Pharmacology, UCL, London WC1E 6BT, UK.
Email: d.colquhoun@ucl.ac.uk

Because of the voltage dependence that results from their block by magnesium, their long activations, and their ability to conduct calcium, NMDA receptors are thought to be important in the central nervous system (Dingledine *et al.* 1999; Cull-Candy *et al.* 2001; Erreger *et al.* 2004). A hallmark of synapses that contain NMDA receptors is the prolonged depolarizing current that results from their activation. The properties of the receptors which allow them to generate their long and complex activations have recently been investigated by Banke & Traynelis (2003), Popescu *et al.* (2004), Erreger *et al.* (2005) and Auerbach *et al.* (2005), but are still not completely understood. We have tried here to combine recent advances in the understanding of the structure, gating and of the modulation of the NMDA receptors to produce a structurally based mechanism for their behaviour.

Most receptors respond to a brief pulse of agonist with a few brief openings in quick succession, the whole activation lasting for only a few milliseconds. In contrast, NMDA receptors produce activations of widely varying length, but with a slow component (which carries most of the current and therefore dominates the synaptic current) that lasts roughly 100–200 ms, in the case of the NR1/NR2A receptor (Wyllie *et al.* 1998; Banke & Traynelis, 2003). The idea of a single 'activation' was defined, for receptors that have only one agonist, as the visible events that occur between the time that the receptor first becomes occupied by an agonist molecule and the time when the last agonist molecule dissociates. In the case of the NMDA receptor this definition must be modified slightly because there are two agonists. If one agonist is present at low concentration and the other is at a high concentration, an activation can be defined as the visible events that occur between the time that the receptor first becomes occupied by the low-concentration agonist and the time when the second low-concentration agonist dissociates. Since one agonist alone can produce no detectable response, this second dissociation ends the activation. In either case, the 'activation' is the physiological event that underlies synaptic currents (Wyllie *et al.* 1998). Individual activations of an NMDA (NR1/NR2A) receptor have a far more complex structure than nicotinic or glycine receptors. They have *at least* two open time components and four shut-time components

 DOI: 10.1113/jphysiol.2005.095349

(Gibb & Colquhoun, 1992; Wyllie *et al.* 1998; Banke & Traynelis, 2003). Even more strikingly, rather than being open for about 98% of the time during an activation, as for nicotinic (Colquhoun & Sakmann, 1985) and glycine (Beato *et al.* 2002, 2004; Burzomato *et al.* 2004) receptors, they are shut for as much time as they are open during an activation. Determining what underlies this complexity of gating is the first hurdle to understanding how NMDA receptors work.

The second hurdle has been the fact that the structure of the receptor, until quite recently, was undetermined. Physically based schemes for binding and gating require some knowledge of the number and possibly the arrangement of subunits within a receptor. Several recent studies now seem to confirm that NMDA receptors are composed of two NR1 and two NR2 subunits arranged as a dimer of dimers around the pore (Schorge & Colquhoun, 2003; Banke & Traynelis, 2003). This proposed structure provides a basis for development of functional mechanisms.

The third reason why NMDA receptors have been so difficult to study is that their function can be modified in many ways. It has been claimed that NMDA receptors can interact with more than 70 intracellular proteins (Husi *et al.* 2000), though it is not known how many of these have any important effect on their function. Extracellular calcium, magnesium, zinc and hydrogen ions certainly affect receptor function (Johnson & Ascher, 1990; Paoletti *et al.* 1997; Low *et al.* 2000). This host of regulators make it almost impossible to investigate the NMDA receptor under physiological conditions. Most experiments have been done in roughly physiological concentrations of calcium and hydrogen ions, but in the nominal absence of magnesium and zinc ions. Although it is relatively easy, if unphysiological, to eliminate magnesium ions, trace contamination with zinc may be more important than has been appreciated.

In this paper we attempt to exploit the recent resolution of the order of subunits in the NMDA receptor, recent proposals about the gating of the receptors and studies of the effects of ions, to develop and fit a mechanism for the actions of glutamate and glycine that has a structural basis.

Methods

Expression of NR1a/NR2A receptor channel cRNA for each of the NMDA receptor subunits was done as we have already described (Béhé *et al.* 1995; Wyllie *et al.* 1996; Wyllie *et al.* 1998). Oocytes were obtained from *Xenopus laevis* that had been anaesthetized by immersion in a 0·2% solution of tricaine (3-amino-benzoic acid ethyl ester), decapitated and pithed. Oocytes were defolliculated and injected with cRNA coding for NR1a and NR2A subunits (see Béhé *et al.* 1995 for details). The vitelline membrane of each oocyte was removed before making patch-clamp recordings. Oocytes were used 3–10 days after injection with cRNA.

Steady-state recordings of single channel activity

Low concentration (5–200 nM glutamate) recordings of recombinant NMDA channel activity in outside-out patches, held at −100 mV, unless noted otherwise, were made in an external solution containing (mM): 125 NaCl, 3 KCl, 1.25 NaH_2PO_4, 20 Hepes and 0.85 $CaCl_2$ (pH 7.4 with NaOH). A free calcium concentration of 0.85 mM is equivalent to 1 mM total calcium in a bicarbonate buffer, as used in our earlier experiments on native NMDA receptors. Patch-pipettes were made from thick-walled borosilicate glass (GC150F, Clark Electromedical, Reading, UK) and filled with an 'internal' recording solution that contained (mM): 141 potassium gluconate, 2.5 NaCl, 10 Hepes and 11 EGTA (pH 7.4 with KOH). These solutions were chosen so that the reversal potential of K^+ and Cl^- ions was −100 mV. After fire-polishing of their tips, pipettes had resistances of 8–15 MΩ Single channel currents were recorded with an Axopatch-1D amplifier (Axon Instruments) and stored on digital audio tape (DAT) for subsequent analysis.

We have here, as in past work, found that magnesium ions can be eliminated effectively by using ultra-pure reagents and Hepes-based external solutions (Béhé *et al.* 1995; Wyllie *et al.* 1998). If contamination did occur, the effect was obvious: records that had obviously shortened open times were discarded from further analysis. No additional precautions were taken to eliminate zinc, and records that we suspected of having trace zinc contamination (empirically described as 'low P_{open}' records, and judged using the criteria described in Results, below) were separated from records which did not show these effects. The composition and naming of solutions are summarized in Table 1.

Data were filtered at 2 kHz and sampled at 20 kHz. Analysis of channel activity was essentially as described in Hatton *et al.* (2003). After creating an idealized list of open times, shut times and amplitudes, by time course fitting with SCAN (Colquhoun & Sigworth, 1995), the EKDIST program was used to inspect stability plots, and, for stable experiments, to fit distributions of amplitudes, shut times, open period duration and various sorts of burst properties, in the usual way (Colquhoun & Sigworth, 1995). An apparent open period is defined as a period when the channel appears to be continuously open (regardless of amplitude); often it will be extended by missed brief shuttings. A resolution of 45 μs was imposed retrospectively on the idealized data before fitting distributions.

Bursts of openings were defined as groups of openings, each group being separated by apparent shut times longer than a specified duration, t_{crit}. The value of t_{crit} was

Table 1. Composition of solutions

Solution description	[Glu]	[Gly]	pH	$[Ca^{2+}]$	[EDTA]
1 low [glu + gly]	50–300 nM	50–300 nM	7.4	0.85	0
2 low [glu]	50–200 nM	10–100 μm	7.4	0.85	0
3 low [gly]	10–100 μM	50–200 nM	7.4	0.85	0
4 high [glu + gly]	100 μM	100 μM	7.4	0.85	0
5 pH 8.0, high [glu + gly]	100 μM	100 μM	8.0	0.85	0
6 EDTA 7.4, high [glu + gly]	100 μM	100 μM	7.4	0	1
7 EDTA 8.0, high [glu + gly]	100 μM	100 μM	8.0	0	1

All solutions contained the following ingredients, but varied in pH, Ca^{2+} concentration and EDTA concentration as shown in the table.

generally chosen between the 4th and 5th components of the shut-time distribution which, in the patches that were used, differed in time constant by a factor of around 100-fold. This is sufficient separation to divide the record into activations, or 'superclusters', with less than 1% of shut times being misclassified. In patches with less than 200 nM of either glutamate or glycine, t_{crit} defined groups of openings that were separated by long shut times that contained one (or more) sojourns in which the binding sites for one of the agonist were in the unliganded state; the groups of openings so defined were, to a good approximation, 'activations' of the receptor, as defined above. Such groups of openings are referred throughout as 'superclusters' (to distinguish them from the shorter groupings, or 'bursts', that can be defined within a single activation (Gibb & Colquhoun, 1992; Wyllie *et al.* 1998). When the concentrations of both agonists are high (above 10 μM), it is not possible to separate individual activations. In long recordings at high concentrations of both agonists, there are some long shut times that result from sojourns in desensitized states, but they were too infrequent to be included in our mechanism. In one extreme case, only one long shut time was present in over 10 000 fitted events. On average the long shut times contributed less than 1% to the fitted shut-time distribution in patches with saturating glutamate and glycine. These long shut times were excised from the records, and were not included in the fitting of exponentials (with EKDIST) or the fits (with HJCFIT). Because they were so rare in our data, they were excised before fitting, and our mechanisms do not therefore include any long-lived 'desensitised' states.

Estimation of rate constants with HJCFIT

The distributions of durations were fitted (in EKDIST) with mixtures of arbitrary numbers of exponential probability density functions. For the purposes of understanding the mechanism it is not these arbitrary time constants that are needed, but the rate constants in the postulated receptor reaction scheme, these being (insofar as a realistic mechanism can be postulated) the quantities that have a real physical significance. This was achieved by calculating, from the postulated mechanism, the likelihood of the entire sequence of apparent open and shut times, in the order in which they occur. The order matters, because open and shut times are correlated, so the probability of seeing a specified open time depends on the length of the adjacent shut time. The calculation of the likelihood has to use joint distributions that take this into account (Colquhoun *et al.* 1996). There are many brief events (especially brief shuttings) that are too short to be resolved, so the open-time distributions given by, for example, Colquhoun & Hawkes (1982), which assume perfect resolution, cannot be used. Instead we have to use distributions (described as HJC distributions) that describe the apparent open and shut times that we actually observe. An exact solution to the problem was found by Hawkes, Jalali and Colquhoun (Hawkes *et al.* 1990, 1992; Jalali & Hawkes, 1992*a*,*b*; Colquhoun *et al.* 1996). This exact solution of the missed event problem is used by the program HJCFIT to calculate the likelihood of the entire sequence of *apparent* open and shut times, and to adjust the values of the rate constants in the mechanism so as to maximize this likelihood. This method, and its use to fit simulated data, was illustrated by Colquhoun *et al.* (1996) where full details of the method can be found (see also Colquhoun & Hawkes, 1995; Colquhoun *et al.* 2003; and the HJCFIT program manual online).

NMDA channels, recorded under our conditions, still show subconductances of the sort reported by Béhé *et al.* (1995), as shown in Fig. 4*C*. The subconductances make up a small proportion (less than 15%) of all openings, and it is beyond our scope to try to incorporate them into a reaction mechanism, so they were ignored, in the sense that any period for which the channel appeared to be continuously open was treated as an opening, even if it happened to contain a subconductance level.

When more than one channel is present, the shut time between one activation and the next will be shorter (on average) than if only one channel were present. This means that the record must be divided into groups of openings such that all the openings in each group come, almost certainly, from one individual channel. The likelihood can then be calculated separately for each such group, and the overall likelihood, which is what is maximized, is found as the product of all the group likelihoods. At

low concentrations of one or both agonists, the groups will be much the same as individual channel activations, though for the purposes of fitting this does not matter; all that matters is that all openings in the group are from the same channel. The grouping is done by specifying a critical shut time, t_{crit}. The interval between two such groups of openings cannot be used directly for fitting because the second group could originate from a different channel from that which gave rise to the first group. However, some information can be recovered because we do know that the true shut time between the end of the first group and the start of the next group *from the same channel* must be *at least* t_{crit}. This knowledge is used in the calculation of the likelihood for each burst by using the initial and final vectors defined by Colquhoun *et al.* (1996, eqns 5.8 and 5.11), and these will be called CHS vectors. Simulations show that their use is important when fitting short bursts in low concentration records (Colquhoun *et al.* 2003). For all agonist concentrations apart from high [glu + gly] (see Table 1) it was considered that desensitization (which is not included in our models) would be sufficiently unimportant that CHS vectors should be used for fitting.

Simultaneous fits with HJCFIT

For the fitting of rate constants to (idealized) data, several patches (usually between 3 and 10), at different concentrations of glutamate and glycine, were fitted simultaneously. In no case were patches with different pH, EDTA or $[Ca^{2+}]$ pooled together, because the influence of these agents was not incorporated explicitly into our models.

Unless otherwise stated, means are given together with the standard deviation of the mean (S.D.M., also known as the standard error S.E.M.), or with the coefficient of variation of the mean (C.V.M.) expressed as a percentage of the mean.

The HJCFIT program, and all other programs used here, can be obtained from http://www.ucl.ac.uk/Pharmacology/dc.html.

Results

Patch to patch variability in open probability

Some patches recorded in the presence of saturating concentrations of both agonists (100 μM glutamate, 100 μM glycine) showed variability over time, as illustrated in Fig. 1*A*. During the period shown the probability of the channel being open (P_{open}) was low at first but then switches to higher P_{open}. A stability plot for P_{open} for this sort of patch (Fig. 1*E*, grey) shows fluctuations, with P_{open} being between 0.1 and 0.6 for most of the time. Other patches, such as the trace illustrated in Fig. 1*B*, recorded under similar conditions, showed a higher and stable P_{open} as shown by the stability plot in Fig. 1*E* (black).

Recent work has shown that both zinc ions and hydrogen ions, in nanomolar concentrations, increase the area of a relatively long (10–20 ms) component of the shut-time distribution (Erreger, 2002). When recording in nominally zinc-free conditions, we found that some of our patches had a 10–20 ms shut-time component that was prominent relative to the 0.3 and 2 ms components seen in zinc-free conditions. When this component represented more than 10% of the shut times in the distribution, the single channel trace showed long stretches in which the probability of the channel being open (P_{open}) was low, as illustrated in Fig. 1*A* and *E* (grey). For example, Fig. 1*C* shows the shut-time distributions for two patches both recorded with nominally identical solutions 0.85 mM $[Ca^{2+}]$, pH 7.4, 100 μM glutamate and 100 μM glycine (solution 4 high [glu + gly], see Table 1). The distribution in grey is from a patch that had long stretches with a low P_{open}, even though it was recorded in the presence of saturating concentrations of both agonists (as in Fig. 1*A*). In contrast, the patches which had a small proportion (less than 10%) of the 10–20 ms shut-time component, shown in black in Fig. 1*C*, had much more stable gating over time, and lacked the low-P_{open} stretches, as in Fig. 1*B* and *E* (black histogram).

The distributions of apparent open times also differed between the two sorts of patches just described. Patches with little or no '10–20 ms' shut-time component required only two components to fit the distribution of apparent open times ('open periods' see Methods), as shown in Fig. 1*D* (black) and Table 2. On the other hand, those patches that had a prominent '10–20 ms' shut-time component, and showed low-P_{open} gating, often required three open-time components for a good fit (Fig. 1*D*, grey).

We found that flushing the perfusion system and chamber regularly with 10 μM–1 mM EDTA reduced dramatically the '10–20 ms' component of the shut-time distribution with respect to the 0.3 and 2 ms components (Fig. 1*C*, black). In addition, the stretches of low-P_{open} gating were virtually eliminated (Fig. 1*E*, black). Any patch was discarded from further analysis during this project if (a) it needed more than 10% of the 10–20 ms component to fit its shut-time distribution, or (b) it needed three components to fit its open-time distribution. These patches were not only unlikely to be fitted by a single kinetic mechanism (as they went through distinct changes in their gating over time, e.g. from high to low P_{open}), but also had very different open-time distributions from the stable patches with low proportions of the 10–20 ms shut times. Records that differ qualitatively (at the same agonist concentrations) obviously cannot be fitted simultaneously with a single mechanism.

The selection criteria resulted in exclusion of 5 out of 21 patch recordings at pH 7.4 and Ca^{2+} at 0.85 mM. The remaining 16 patches were used for analysis. It is possible that the long stretches with low P_{open} may represent times when zinc is bound to the channel, so

enhancing inhibition by hydrogen ions (Low *et al.* 2000). We did not examine this question systematically, and further work will be needed to test it. For our present purposes the explanation for unstable behaviour is not crucial. What matters is that records that are fitted behave consistently.

Intracellular proteins and second messengers

Although NMDA receptors are thought to react with many intracellular proteins (Dingledine *et al.* 1999; Husi *et al.* 2000; Rycroft & Gibb, 2004), very little is known about the effects of these interactions on the function of the channel. Such interactions have been suggested as a possible reason for the 'modal' behaviour that was observed in cell-attached patches from transfected HEK cells by Popescu & Auerbach (2003). In the absence of extracellular Ca^{2+}, and in the presence of 1 mM extracellular EDTA, they found that the NMDA receptor channel switched between distinct modes of gating on a time scale of seconds. These switches were characterized by changes in the open probabilities and open-time durations, and the authors postulated that these dramatic switches between modes might reflect intracellular modulation of the NMDA receptors occurring during the recordings.

In contrast, we did not observe this modal behaviour when recording from outside-out, rather than cell-attached, patches under similar extracellular conditions (1 mM EDTA, pH 8, no Ca^{2+}) and our standard intracellular solutions (with 10 mM EGTA). A recording under these conditions is shown in Fig. 2. We never saw modal gating, even in the longest recordings.

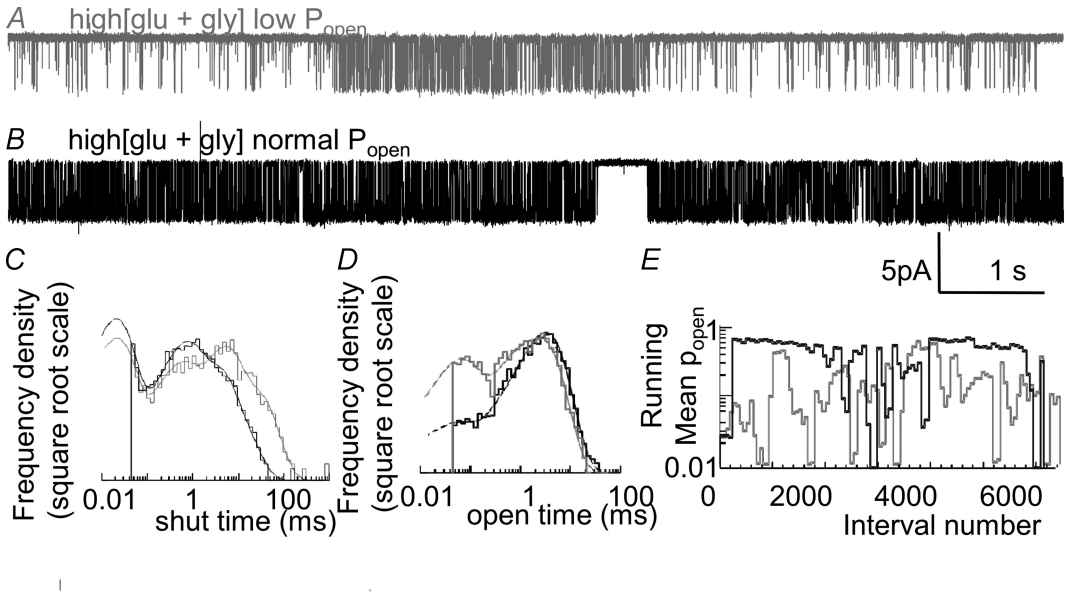

Figure 1. Some patches recorded with saturating concentrations of both glutamate and glycine have stretches of low P_{open} and altered open and shut-time distributions
All recordings were made with the solution labelled high [glu + gly] (solution 4, see Table 1). Openings are downwards in this and subsequent records. *A*, recording in 100 μM glutamate and 100 μM glycine with nominally zinc-free conditions. This record has stretches in which P_{open} is quite low. *B*, another recording, made under the same nominal conditions as that in *A*, but this record has a high, stable P_{open}. *C*, shut-time distributions from two patches, both recorded in high [glu + gly] as in *A* and *B*. The grey data and fits are from a patch which was excluded because the 10–20 ms component represented more than 10% of the shut-time distribution (i.e. data resembling those in *A*). The black data and fits are from a patch which had a stable P_{open}, and in which less than 10% of the shut-time distribution came from the 10–20 ms component (i.e. data like those in *B*). Note the shift in prevalence of shut times in the 10–100 ms range. The black histogram contains 3004 events, and the grey contains 3431. *D*, open period distributions from the same two patches that are shown in *C*. The grey data correspond to the patch which was excluded on the basis of excessive 10–20 ms shut times. The black data are from the patch with relatively few 10–20 ms shut times. The data from the unstable patch (grey) show the large increase in short events (relative to the number of long events) often seen in these patches, while in the stable patch (black) there are relatively fewer short (below 1 ms) open periods. The black histogram contains 3003 events, and the grey contains 3430. *E*, stability plots for P_{open} in the same two patches, showing the variable P_{open} (grey) of the discarded patch and the stable P_{open} (black) from the patch with relatively few 10–20 ms shut times. The means were calculated with a sliding window of 50 events calculated in steps of 25 events. The mean P_{open} in the stable patch (black) is about 0.6, but the unstable patch (grey) rarely reaches this level, and is much more variable. Occasional drops in the stable (black) running mean are the result of individual long, presumably desensitized, shut times (over 100 ms), rather than 10–20 ms shut times.

Table 2. Distributions of shut times within superclusters, and of open times, in various solutions

		Shut 1		Shut 2		Shut 3		Shut 4		t_{crit}	Open 1		Open 2	Open 3 (low P_{open} only)	
		τ_1 (μs)	Area (%)	τ_2 (ms)	Area (%)	τ_3 (ms)	Area (%)	τ_4 (ms)	Area (%)	(ms)	τ_1 (μs)	Area (%)	τ_2 (ms)	τ_3 (ms)	Area (%)
Low [glu + gly]	Mean ($n = 3$)	19.4	53.0	0.35	13.6	1.88	19.7	7.8	7.17	37.0	61.6	18.6	3.42	—	—
	S.D.M.	0.6	8.1	0.05	1.7	0.21	2.9	1.8	1.68	4.6	3.7	4.3	0.57	—	—
Low [glu]	Mean ($n = 3$)	21.5	43.8	0.32	14.2	1.72	32.2	12.5	4.60	35.9	52.7	10.1	3.00	—	—
	S.D.M.	0.8	1.9	0.05	2.7	0.20	0.3	3.3	1.61	4.4	8.1	3.0	0.39	—	—
Low [gly]	Mean ($n = 4$)	23.6	46.0	0.46	18.2	2.74	24.7	13.8	5.00	51.7	67.5	14.7	3.37	—	—
	S.D.M.	3.8	8.5	0.10	4.2	0.58	3.1	4.2	1.03	12.9	7.1	4.6	0.37	—	—
High [glu + gly]	Mean ($n = 4$)	19.3	49.3	0.58	22.5	2.88	20.1	15.4	7.20	*n.a.*	63.5	12.7	3.18	—	—
	S.D.M.	2.3	6.4	0.09	4.8	0.77	2.6	3.9	1.08	*n.a.*	9.1	2.6	0.13	—	—
High [glu + gly], low P_{open}	Mean ($n = 4$)	18.6	38.3	0.37	13.5	3.19	28.5	19.5	18.45	*n.a.*	50.3	28.6	2.57	0.78	15.4
	S.D.M.	1.7	4.5	0.03	3.5	1.16	3.2	4.4	1.33	*n.a.*	4.4	2.9	0.04	0.22	3.3
pH 8, high [glu + gly]	Mean ($n = 4$)	16.7	54.1	0.30	14.4	2.23	26.4	11.8	4.88	*n.a.*	70.7	8.8	3.15	—	—
	S.D.M.	1.6	4.0	0.10	2.5	0.61	2.2	4.7	1.26	*n.a.*	18.1	1.9	0.26	—	—

The absence of modes in our outside-out patches supports the hypothesis proposed by Popescu & Auerbach (2003) that the modal gating they observed in cell-attached patches might be a result of slow changes in the properties of the channel produced by effects of intracellular components that are absent in outside-out patches. Recently Auerbach *et al.* (2005), using oocyte transfection as here, also observed recordings without modes, under similar conditions: they suggested that the modal behaviour was dependent on the transfection system.

The conditions we used for routine recordings (outside-out patches, recorded in set-ups regularly flushed with EDTA, and with intracellular EGTA) seem sufficient to prevent many of the factors which normally modulate the gating of NMDA receptors. Under these conditions it becomes feasible to investigate receptor mechanisms that involve only the two agonists, glutamate and glycine, and the receptor itself, in an attempt to explain the behaviour of the NMDA receptors.

The role of glycine

Glycine is a necessary co-agonist for NMDA receptor gating (Johnson & Ascher, 1987; Kleckner & Dingledine, 1988). However, little work has been done at the single channel level to compare the role of glycine with that of glutamate in controlling the behaviour of the channels. Macroscopic work has shown that the presence of glycine suppresses one form of desensitization in a manner consistent with the binding of glycine reducing the affinity of glutamate for its binding site (e.g. Nahum-Levy *et al.* 2001).

Recently, the separate roles of glycine-dependent and glutamate-dependent gating have been examined using partial agonists at a single channel level (Banke & Traynelis, 2003). Analysis of partial agonists for either the glutamate or the glycine site on receptors containing NR1 and NR2B led to the suggestion that the gating of NR1 and NR2B subunits may underlie two distinct shut-time components within activations. This work has led to a promising, but simplified, model of the fully liganded gating behaviour of NR1/NR2B-containing channels (shown in Fig. 5*C*) The model is simplified because in their work, only one component was resolved in the open-time distribution, and the binding of each agonist was not considered explicitly.

Our results imply the presence of at least two open states, so we had to extend these models. Recently, Erreger *et al.* (2005) have also seen two-component distributions of open time for NR1/NR2A channels. A possible explanation of the multiple open times seen in the distribution is that the shorter open-time constant might reflect the gating of channels that are not fully liganded. That, at least, seems to be the case for both nicotinic and glycine receptors (Colquhoun & Sakmann, 1981, 1985; Beato *et al.* 2002, 2004; Burzomato *et al.* 2004). To test whether the multiple open times in the distribution from NR1-1a/NR2A channels originated, similarly, from partially liganded channels, we investigated their behaviour in different concentrations of glutamate and glycine.

Work from several groups indicates that the NMDA channels, and all glutamate receptor ion channels, contain four agonist binding sites (Benveniste & Mayer, 1991; Clements & Westbrook, 1991; Banke & Traynelis, 2003; Schorge & Colquhoun, 2003), two for glutamate and two for glycine. Work with tandem constructs suggests that they are probably arranged as a dimer of dimers (Schorge & Colquhoun, 2003). This work agreed with early jump experiments using NMDA receptors isolated from cultured neurones (Benveniste & Mayer, 1991; Clements & Westbrook, 1991). These experiments were also interpreted as meaning that two molecules of glutamate and two molecules of glycine must bind before the channel opens.

If a channel with any fewer molecules of either agonist bound were able to open, then these partially liganded channels would almost certainly contribute a component to the open-time distributions. For example, channel openings that occurred with one, or no, glycine molecules

bound, would be likely to stay open for a shorter time (or re-open less often) than channels that have all binding sites occupied. If this were the case then recordings done with very low glycine concentrations should have an excess of the shorter open states. Likewise if the short openings arose from channels which are not fully saturated with glutamate, then recordings done with very low glutamate should have an excess of the short openings, compared with channels recorded in saturating glutamate and glycine concentrations.

To test the hypothesis that partially liganded openings contribute to the shorter component of open-time distributions, we made recordings in very low glycine (50–300 nM) with saturating glutamate (10–1000 μM), or very low glutamate (50–300 nM) with saturating glycine (10–1000 μM). For comparison we also made recordings with both agonists saturating (10–1000 μM), and both agonists at very low concentration (50–300 nM). Under all four conditions the distributions of open periods were remarkably similar (Table 2, Fig. 3). This observation is quite different from what is seen with nicotinic (Colquhoun & Sakmann, 1981, 1985) or glycine receptors (Twyman & Macdonald, 1991; Beato *et al.* 2002, 2004; Burzomato *et al.* 2004). When both agonists were applied at very low concentrations, the area of the shortest open-time component may have been slightly higher, but the difference from other concentrations does not approach statistical 'significance' ($P \geq 0.27$, depending on which concentrations are compared; Student's *t* test).

This lack of any detectable concentration dependence, suggests that receptors cannot open with less than all four binding sites occupied.

Partially liganded openings were not detected either in the macroscopic jump experiments reported previously (Benveniste & Mayer, 1991; Clements & Westbrook, 1991), though this is inconclusive because, at least in the case of the nicotinic receptor, the amount of current carried by monoliganded openings is too small to be detected in macroscopic jump experiments.

There is also a theoretical possibility that partially liganded openings have much the same mean open time as fully liganded openings, but the precedents speak against this, and in any case, if that were true, the open-time distributions should have only one component, which is not so. Another theoretical possibility is that partially liganded receptors could access the same two open states, with the same relative frequency, that are accessed by fully liganded receptors. Again there is no precedent for such behaviour in either nicotinic or glycine receptors, but it is mentioned for completeness.

Correlations between neighbouring open and shut times

Gibb & Colquhoun (1992) observed (with hippocampal NMDA receptors) that long openings tend to be next to short shut periods, and short openings are more likely to be adjacent to longer shut times. This type of behaviour is also observed in muscle nicotinic receptors (e.g. Colquhoun & Sakmann, 1985; Hatton *et al.* 2003) and in glycine receptors (Beato *et al.* 2002, 2004; Burzomato *et al.* 2004). The existence of these correlations provides information on the connections between the various states of the receptor (Fredkin *et al.* 1985; Colquhoun & Hawkes, 1987; Blatz & Magleby, 1989). In the cases of both nicotinic and glycine receptors, the physical explanation of the correlations depends on the existence of partially liganded openings that are shorter than fully liganded openings (a difference that is exaggerated by the failure to detect some of the brief shuttings that separate re-openings of the fully liganded receptor). The partially liganded openings are, on average, brief, and after one has occurred the channel is unlikely

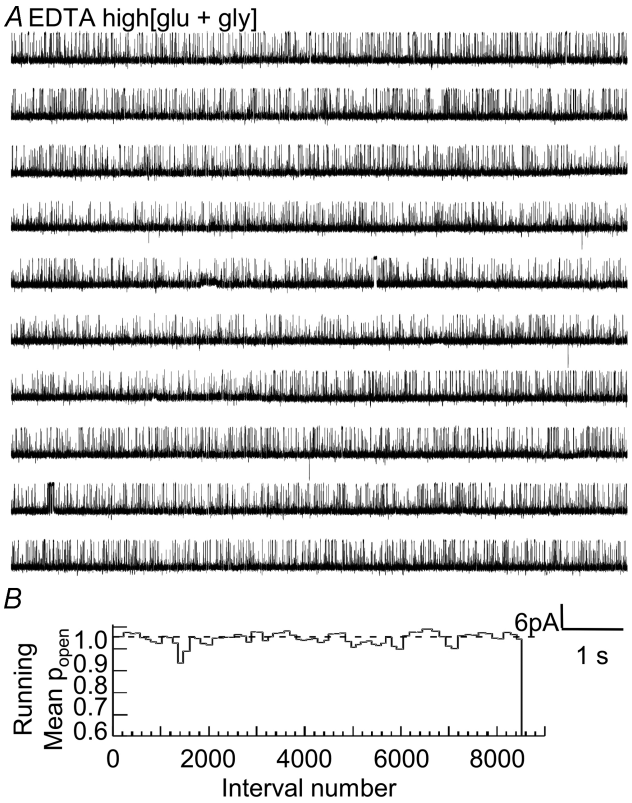

Figure 2. Outside-out patches do not show modal behaviour in the presence of EDTA

A, representative patch recorded in pH 8.0, 1 mM EDTA, high [glu + gly] (very low calcium and hydrogen ion concentrations; solution 7 in Table 1). The behaviour of the channel was uniform with no obvious modal switches. This was tested in four separate patches, each lasting longer than 10 min. The traces represent 100 s of continuous recording. Some patches (though not the sample shown here) had occasional very long shut times (often longer than 1 s), which presumably arose from desensitized states. *B*, running average (stability plot) of P_{open} from same patch as shown in *A* (for first 8500 events only). In these conditions the mean P_{open} is high (about 0.95, note the ordinate in this case). The P_{open} is also remarkably stable over the 8500 transitions shown here.

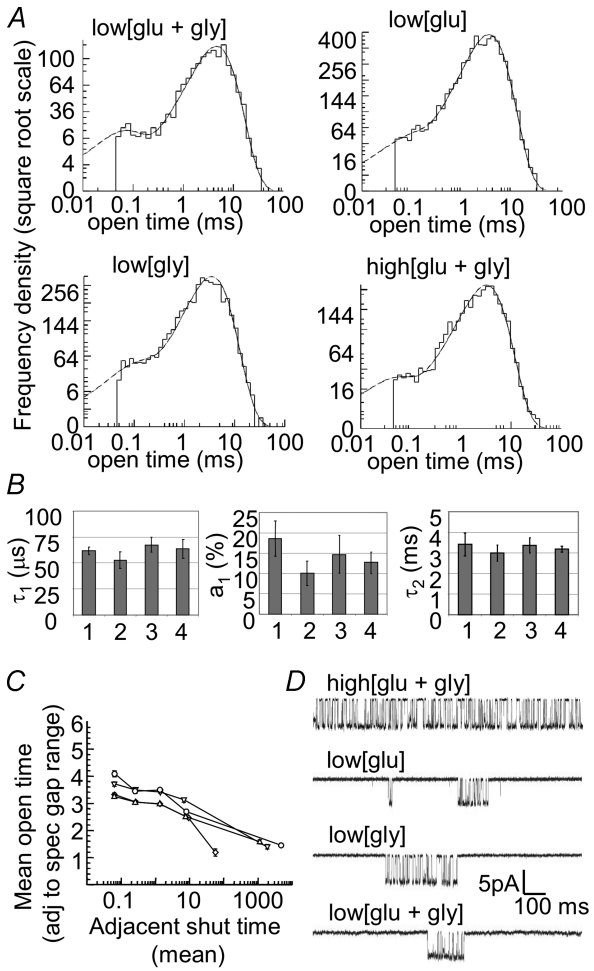

Figure 3. Open period distributions at different concentrations of glutamate and glycine

A, representative open period distributions from patches recorded with four different glutamate and glycine concentrations, solutions 1–4 as specified in Table 1 (pH 7.4, with 0.85 mM Ca^{2+}, no EDTA). These were from patches with stable P_{open} (as in Fig. 1*B*) and less than 10% of their shut-time distributions fitted by the 10–20 ms component. Here and in other pooled data 'low' indicates a concentration of glutamate or glycine of 50–300 nM, and 'high' indicates a concentration greater than 10 μM (see Table 1). *B*, comparison of time constants (τ) and relative contribution (area of the τ_1 component, a_1 (%)) of the two open-time components for all four agonist combinations. These histograms show values (mean ± S.D.M., $n = 3$–4 patches for each combination) from pools of patches recorded in different glutamate and glycine concentrations. Although the values are somewhat variable there is no distinct trend in the open-time rates or components with changes in either glutamate or glycine concentration. *C*, the observed relationship between mean apparent open period and the adjacent apparent shut times for pooled patches at different concentrations of glutamate and glycine, calculated as described in the text. The data for the high [glu + gly] patches are plotted only up to 100 ms because these records contained few shut times longer than that. In all agonist concentrations, long open periods tend to be adjacent to short shut times, whilst shorter open periods are near long shut times. However, the trend is not affected by the concentration of either or both agonists, suggesting that it is not dependent on the agonist binding. All data are with 0.85 mM [Ca^{2+}], pH 7.4 (see Table 1 for details). *D*, representative 'superclusters' from patches recorded with different concentrations of glutamate and glycine. All four traces are recorded in 0.85 mM [Ca^{2+}] at pH 7.4 (see Table 1). The trace shown for high [glu + gly] ends arbitrarily, whereas the other three traces show an individual supercluster of activity separated by long shut times above the t_{crit} (calculated between the 4th and 5th shut-time component in each individual patch). In the patches other than high [glu + gly], these bursts should be good approximations to single activations of the channel (see text).

to re-open, so (at low concentrations) the short opening will usually be followed by a long shut time. Fully liganded openings, on the other had, are on average longer, and the fully liganded channel will often re-open after a very brief shut time (thus generating the characteristic fully liganded bursts of openings), so the longer openings will often be adjacent to short shut times. At high agonist concentrations, where few partially liganded openings are expected, correlations vanish (Beato *et al.* 2002, 2004; Hatton *et al.* 2003; Burzomato *et al.* 2004).

The behaviour of NMDA receptors is quite different from that of nicotinic and glycine receptors. The evidence so far suggests that we cannot detect partially liganded openings, and although the records show a negative correlation between open time and adjacent shut times that is superficially similar to that seen with nicotinic and glycine receptors, this correlation is essentially unchanged when both agonists are present in saturating concentrations. This is demonstrated in the experiments shown in Fig. 3*C*. Figure 3*C* shows conditional mean open-time plots under four different concentration conditions. Openings were selected according to the length of the shut times adjacent to them (both preceding and following shut times were used for each opening, as is appropriate when microscopic reversibility is obeyed). The shut times were divided into five groups depending on their duration: 0.045–0.1 ms, 0.1–3.0 ms, 3.0–20.0 ms, 20–100 ms and longer than 100 ms. For each of these ranges of shut times, the average of the adjacent open times is calculated. The mean open time, conditional on the opening being adjacent to a shut time in the specified range, was then plotted against the mean of the shut times in that range. The same ranges of shut times were used for all four concentration conditions: low [glu + gly] (50–300 nM), high [glu + gly] (10–1000 μM), low [gly] and low [glu] (see solutions 1–4 in Table 1 for complete solutions). In all the different mixtures of agonists, the relationships between the mean duration of open times and their adjacent shut times are remarkably similar. The relationship has virtually no dependence on the concentration of either agonist. This suggests that the correlation between open time and adjacent shut times does not arise from partially liganded states, as such a correlation would be lost during exposure to high concentrations of agonist, as is seen for both nicotinic and glycine receptors. The persistence of these correlations in

Table 3. Properties of superclusters of openings in different concentrations of glutamate and glycine

	Patches (*n*)	Bursts with single openings (%)	Number of bursts	Mean length (ms)	S.D.	S.D.M.	Mean open time (ms)	S.D.	S.D.M.	Mean P_{open}
Low [glu + gly]	3	0.49	243	85.8	353	22.6	54.3	274	17.6	0.63
Low [glu]	2	0.44	279	108	185	11.1	68.4	125	7.50	0.63
Low [gly]	3	0.55	296	126	282	16.4	76.4	196	11.4	0.61
High [glu + gly]	4	0.34	*83	583	1060	116	268	557	61.1	0.46
pH 8, high [glu + gly]	4	0.43	*39	822	1000	160	428	524	83.9	0.52

*The intervals between clusters in saturating concentrations of both agonists result from periods in which all channels are desensitized. In contrast, when one or both agonists is present at a very low concentration, these intervals represent predominantly periods during which there are one or more sojourns in states with the binding sites for one of the agonists unoccupied.

all agonist concentrations provides additional evidence that the NMDA channels do not open when partially liganded. It seems that correlations arise from fully liganded receptors. Thus, the fully liganded channels must have more than one open state, and more than one shut state, and these states must be connected in a way that allows correlations to arise. One way of putting this is to say that it must not be possible to separate open states from shut states completely by deleting a single shut (or open) state, i.e. there must be more than one 'gateway state' (Fredkin *et al.* 1985; Colquhoun & Hawkes, 1987; Blatz & Magleby, 1989).

Activations and super clusters

We have defined a single 'activation' of an ion channel as the visible part of what happens between the time that the first agonist molecule binds and the time that the last agonist molecule dissociates, leaving the receptor in the completely unliganded state (Edmonds *et al.* 1995). While any ligands are still bound, the channel may still re-open relatively easily, though the lower the concentration the less likely this will be. At sufficiently low agonist concentrations, the individual activations will be separated by long shut times, during which the receptor spends one or more sojourns in the unliganded state. Thus the superclusters of openings that constitute an individual activation can be distinguished from each other with good accuracy. Activations were measured with native NMDA receptors by Gibb & Colquhoun (1992), and with recombinant NMDA receptors by Wyllie *et al.* (1998). The activations, which are often long, were termed super-clusters in their work. Similar measurements have been made in muscle nicotinic receptors (Colquhoun & Sakmann, 1981, 1985), and glycine receptors (Beato *et al.* 2002, 2004; Burzomato *et al.* 2004).

Channel activations are interesting from the physiological point of view because synaptic currents (under conditions where the agonist application is brief) are essentially averaged single channel activations, as described by Lester & Jahr (1992) and, quantitatively, by Colquhoun *et al.* (1997) and Wyllie *et al.* (1998). They are also interesting from the mechanistic point of view because it is almost always possible to be sure that all the openings in one activation come from the same individual channel, so their fine structure gives information about the channel's mechanism.

Because of the length of the activations of the NMDA receptor, very low agonist concentrations (usually below 200 nM of either) are needed to achieve clear separation of them. Ideally, the mean shut time between one activation and the next should be several seconds for the NMDA receptor (Gibb & Colquhoun, 1992; Wyllie *et al.* 1998). The ultimate form of low concentration experiment is to observe the single activation that follows a brief pulse of agonist application, when virtually all openings occur at zero concentration so no re-opening is possible once one or other of the agonists has dissociated.

Groups of openings, here called superclusters, were defined in practice by choosing a critical shut time, t_{crit}, such that a shut time longer than this ended a burst. The aim was to define superclusters so that they corresponded as closely as possible to single activations of a channel. Examples of superclusters are shown in Fig. 3*D*. It was, of course, not possible to isolate individual activations when the concentrations of both glutamate and glycine were high. Many patches had to be rejected, either because they showed too much '10–20 ms' component, had short openings (possible magnesium contamination), or simply because the opening rate was too high to allow convincing separation of channel activations, or so low that few activations were recorded. The result was that it was not possible to collect enough superclusters to obtain good quality distributions of supercluster duration, though usually the slow component of this distribution was of the order of 200 ms, similar to our earlier observations (Wyllie *et al.* 1998). Some average properties of superclusters of channel openings are given in Table 3, under three different concentration conditions.

The results in Table 3 show that the probability of being open during a supercluster is almost identical under all three concentration conditions. The average length of

superclusters, and the total open time per burst, are slightly shorter when both agonists are at low concentrations than when one concentration is high, but the difference is far from reaching statistical 'significance'. We can conclude that the channel activations are not very sensitive to the concentrations of either glutamate or glycine, though we certainly could not rule out small effects. This confirms the findings of the brief report by Gibb & Edwards (1991).

The mean P_{open} in these patches, 0.62, is roughly twice the value of 0.36 reported earlier by Wyllie *et al.* (1998). However, some of the open and shut-time distributions in Wyllie *et al.* (1998) show signs of contamination with zinc, and the rather higher P_{open} found here could be a result of selection of only those patches that have a small '10–20 ms' shut-time component.

Full activation of NMDA channels in the presence of EDTA and high pH

In physiological pH and calcium concentrations, but in the nominal absence of magnesium, the maximum attainable P_{open}, in saturating concentrations of both agonists, is far from unity, being 0.3–0.6 (Gibb & Colquhoun, 1992; Wyllie *et al.* 1998; Erreger *et al.* 2005) for NR1/NR2A channels. Therefore it appears that glutamate and glycine, jointly, are partial agonists. However, it may be that the low maximum P_{open} results not so much from the ineffectiveness of the agonists as from block of the channels by hydrogen ions and/or metal ions (Erreger, 2002; Banke *et al.* 2005). Figure 2 showed a record from an outside-out patch with extracellular pH 8.0 and 1 mM EDTA and saturating concentrations of glutamate (100 μM) and glycine (100 μM). Under these conditions the maximum P_{open} is indeed high. For four such patches, the mean P_{open} was 0.88 ± 0.03 (S.D.M.).

These are conditions similar to those used by Popescu & Auerbach (2003) in HEK cells, and by Auerbach *et al.* (2005) in oocytes. Under these conditions, not only would the zinc and magnesium ions be absent, but calcium also is nominally absent, and the hydrogen ion concentration is low. These conditions have an additional dramatic effect on the behaviour of the channels when compared with channels recorded in patches with 0.85 mM calcium and no EDTA. Figure 4*A–C* shows distributions measured on a single patch with saturating glutamate and glycine concentrations, first with EDTA at pH 8.0 (grey data) and then with 0.85 mM calcium and no EDTA at pH 7.4. The addition of EDTA dramatically reduces the average duration of shut times, with the fourth component almost completely lost and the third component also greatly reduced (Fig. 4*A*). The shut-time distribution for patches recorded in the presence of EDTA at pH 8.0 is shifted strongly to shut times with less than 1 ms duration. The fastest shut-time component, with a time constant of about 20 μs, is similar to that seen in the presence of calcium, but the other components of the shut-time distribution cannot be fitted with the same values as the shut times from patches with calcium. Additionally, in the presence of EDTA, the apparent open times are much longer. The main component of the apparent open-time distribution in EDTA is longer than 10 ms compared with about 3 ms in the presence of calcium (Fig. 4*B* and Table 2).

To determine which of these effects were caused by EDTA and which resulted from the change in pH, we subjected the same patch to saturating concentrations of glutamate and glycine at pH 8.0 and 7.4 in the presence and absence of EDTA and calcium. The results are shown in Fig. 4*D–F*. At pH 8.0 with calcium, the durations of the open periods were not much different from those at pH 7.4 with the same calcium concentration, the latter being the conditions used in most of our experiments (Fig. 4*E*). The only noticeable difference was a decrease in the fourth component of the shut-time distribution at pH 8.0 (Fig. 4*D*).

In contrast, exposure to EDTA at pH 7.4 prolongs the apparent open times almost as much as seen at pH 8 with EDTA. The presence of EDTA at pH 7.4 also produced a dramatic change in the shut-time distribution similar to that seen at pH 8.0, although at pH 7.4 there are slightly more longer (about 10 ms) shut times (data not shown).

The amplitude of single channel openings was found to depend on calcium concentration, as has been reported before (e.g. Ascher & Nowak, 1988; Gibb & Colquhoun, 1992; Stern *et al.* 1992; Wyllie *et al.* 1996; Popescu & Auerbach, 2003). In one patch the main level was shifted from 5.3 pA to 6.8 pA when the external solution was switched from pH 7.4 with calcium to pH 8.0 with EDTA. In the recordings in the presence of EDTA, a sublevel was present at about 5 pA, which may correspond to the 4 pA sublevel in the patches recorded in the presence of calcium. However, in the presence of EDTA an additional 'supralevel' was also seen at 8 pA. This new level was also noted in previous work on cell-attached patches from HEK cells (Popescu & Auerbach, 2003). The change was seen only in the presence of EDTA and calcium. No effect on amplitude was seen when the pH alone was changed, either in the presence of EDTA or in the presence of calcium (Table 2) (pH 7.4 with Ca^{2+}, 4.68 ± 0.45 pA, $n = 4$; pH 7.4 with EDTA, 6.56 ± 0.40 pA; pH 8.0 with Ca^{2+}, 5.17 ± 0.20 pA, $n = 4$; pH 8.0 with EDTA, 6.65 ± 0.55 pA, $n = 4$; all mean $\pm$ S.D.M.). This is as expected from the observation by Traynelis & Cull-Candy (1990) that pH does not affect channel conductance.

Unfortunately, because of the large leak current in patches in the presence of EDTA it was not possible to record for long enough from patches in low concentrations of agonists to observe discrete activations of the channel. It was also not possible to determine the EC_{50} values for glutamate or glycine on whole oocytes in the presence of EDTA, again because of the large levels of leak current seen

in these conditions. However, given the level of activity seen under the concentrations of agonists used (100 μM each) it seems that these concentrations must have been close to saturation (see Fig. 2*A*).

Although the conditions the channel is exposed to, in EDTA at pH 8.0, are not at any time expected to occur in the synapses, they do provide a chance to see the gating of the NMDA receptors reduced to the fewest components we have ever observed for this receptor. In the presence of EDTA at pH 8.0 the single channel activity can be described with two clear open-time components and three short shut-time components.

Because of the relative ease of obtaining long recordings over a wide concentration range, as well as because it is closer to physiological conditions, we concentrated most of our efforts on recordings at 0.85 mM Ca^{2+} and pH 7.4, despite the complications of pH sensitivity. These are also the conditions used in most of our earlier work. However, we also analysed records in EDTA at pH 8.0 in an attempt to see whether the same mechanism fitted, and, if so, how the rate constants differed from those in our standard conditions.

Possible mechanisms, based on structural considerations

In the case of nicotinic and, especially, glycine receptors, there is a clear dependence of single channel properties

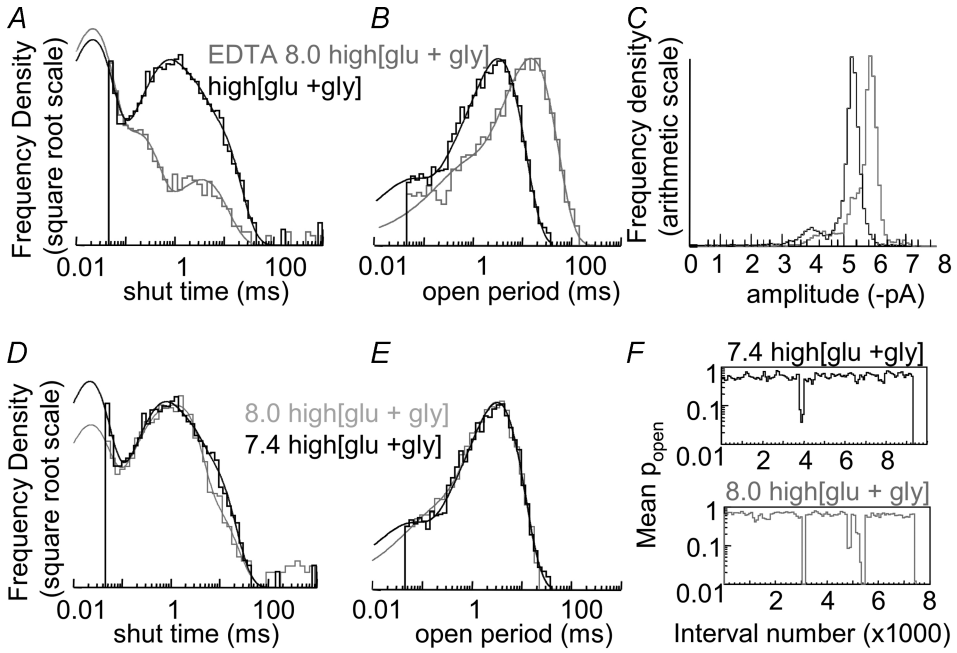

Figure 4. NMDA channel behaviour in the presence of EDTA
All patches were recorded with 100 μm of both glutamate and glycine (high [glu + gly], or solutions 4–7, see Table 1). *A*, shut-time distributions for a single patch recorded in EDTA, pH 8.0 (grey) and in 0.85 mM [Ca^{2+}], pH 7.4 (black). See Table 1 for the complete composition of the solutions. Note the dramatic reduction in shut times over 1 ms long in the presence of EDTA. The black histogram contains 3004 events, and the grey contains 2400. *B*, open-time distributions for the same patches with EDTA, pH 8.0 (grey) and 0.85 mM [Ca^{2+}], pH 7.4 (black). The long component of the open period distributions is shifted from about 3 ms to above 10 ms. The black histogram contains 3003 events, and the grey contains 2399 events. *C*, the amplitudes of individual openings are also changed by the presence of EDTA. While in the presence of calcium (black) NMDA receptors have a conductance of about 50 pS for their main level, and 40 pS for their sublevel, their main level is shifted to 60 pS and the sublevel to 50 pS in the presence of EDTA (grey). In addition a minor 'supralevel' at 70 pS is visible in the presence of EDTA (grey). The black histogram contains 4815 events, and the grey contains 5745. *D–F*, shift in shut-time distributions with change in pH without changing [Ca^{2+}]. A single patch recorded with 100 μm glutamate and glycine at pH 7.4 (black) and pH 8.0 (grey) both with 0.85 mm [Ca^{2+}] (solutions 4 and 5, see Table 1 for details). *D*, raising the pH to 8.0 alone (grey) can decrease shut times longer than about 3 ms, compared with the same patch recorded at pH 7.4 (black). However, the effect of pH alone is not as dramatic as that of EDTA (see Fig. 4*A*). The black histogram contains 3004 events, and the grey contains 2384. *E*, the open period distributions from the same patch used in *D* show that, unlike adding EDTA, elevating the pH to 8.0 in the presence of 0.85 mM [Ca^{2+}] (grey) has little effect on the open-time distribution. The black histogram contains 3003 events, and grey contains 2383 events. *F*, the running averages of P_{open} for the same two patches show that the slight decrease in longer shut times is reflected by an increase in the average P_{open}. The single channel amplitudes were not changed with the change in pH (data not shown).

on agonist concentration. This concentration dependence provides valuable information about mechanisms. In the case of the glycine receptors, the simultaneous fit of several single channel records at a range of agonist concentrations allows good estimates of as many as 18 different rate constants to be made (Burzomato *et al.* 2004). In the case of the NMDA receptor, we not only have to explain channel activations that are more complex than those of nicotinic and glycine receptors, but also the lack of detectable concentration dependence of the channel openings means that there is less information available on which to base the explanation. There is therefore a limit to what we can hope to achieve.

It seems sensible to postulate mechanisms that are based on what is known about structure, if only because rate constants are of interest only insofar as they describe real physical events. We shall presume that the receptor is made up of an NR1 dimer that binds two glycine molecules and an NR2 dimer that binds two glutamate molecules, as suggested by Schorge & Colquhoun (2003), Banke & Traynelis (2003), and Hatton & Paoletti (2005). This means that there must be nine (at least) shut states that are linked by binding steps (including the unliganded and fully liganded states). These are shown in Fig. 5*A*. There must be at least two open states too. Thus macroscopic currents must be described by at least 10 exponential components, of which at most two or three can be resolved. As shown by Wyllie *et al.* (1998), the ability of macroscopic measurements to resolve mechanisms is correspondingly low.

The first model for NMDA channel behaviour, shown in Fig. 5*B*, was developed by Lester & Jahr (1992), with additional binding states for glycine added later (Benveniste & Mayer, 1991; Clements & Westbrook, 1991; Lester *et al.* 1993). This mechanism was postulated before much was known about NMDA receptor structure, on the basis of responses to fast concentration jumps on embryonic hippocampal neurones, in which the NMDA receptors are likely to be mostly the NR1/NR2B type. It provides a good description of the macroscopic behaviour of the channels. It cannot describe single channel results, if only because it contains only one open state, and because it predicts that there will be no correlation between open and shut times.

Banke & Traynelis (2003), in an attempt to account for the complexity of the NMDA receptor activation, postulated that NR1 and NR2 subunits might be able to change conformation separately, and only when both had changed was the channel able to open. The saturated part of one of their mechanisms is shown in Fig. 5*C* (from their Fig. 4). Three lines of argument lend plausibility to this sort of mechanism. Firstly, recent work designed to clarify the structure and stoichiometry of the NMDA receptors (Schorge & Colquhoun, 2003) suggested that the NR1 and NR2A subunits may be arranged as two separate dimers, and it is possible (though not necessary)

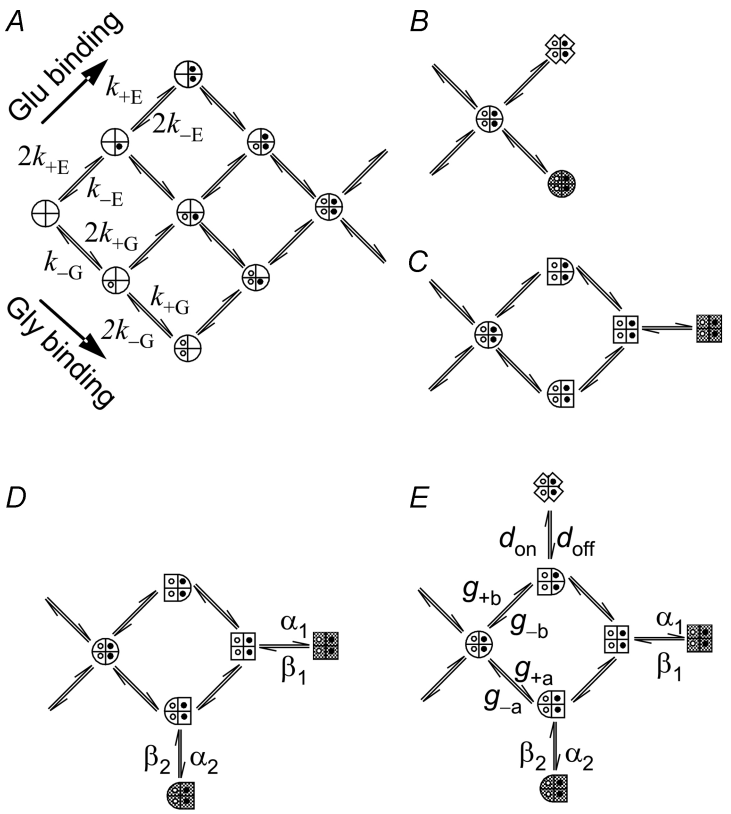

Figure 5. Some of the kinetic schemes proposed by others for NMDA receptors and those tested here using HJCFIT
Circles represent the resting conformation of the receptor; squares represent a flipped (but not necessarily open) conformation; grey denotes an open receptor and an X-shape denotes a shut ('desensitized) state. *A*, the binding states used for all the mechanisms that we fitted. According to the current consensus there are two glutamate-binding NR2 subunits and two glycine-binding NR1 subunits, which give rise to the minimum of 9 states shown here. *B*, the original gating scheme proposed by Lester & Jahr (1992), and modified by Clements & Westbrook (1991) and Benveniste & Mayer (1991). The fragment shown contains only fully saturated receptors. This was combined with much simpler binding schemes than that shown in Fig. 5*A* in earlier work, but Nahum-Levy *et al.* (2001) combined it with the scheme in *A*. *C*, the saturated part of the mechanism proposed by Banke & Traynelis (2003). This was proposed on the basis that NR1 and NR2 might be able to change conformation separately. It still cannot fit our data. *D*, the scheme from Banke & Traynelis (2003) with an additional open state, as required by our results. Although this model was able to fit the open time distributions adequately, it was unable to fit the shut-time distributions in patches recorded with low concentrations of either or both agonists (see Fig. 6). *E*, the final scheme, based on that of Fig. 5*D* but with an additional fully liganded shut state. This mechanism is drawn in full in Figs 7*D* and 10. This mechanism was able to fit the open and shut distributions as well as the correlations seen between open times and adjacent shut times (Fig. 7).

that the two dimers can move separately, as suggested by Banke & Traynelis (2003). Secondly, in the far better defined case of the glycine receptor, the most parsimonious (though not unique) explanation of the single channel observations involves a conformation change that occurs before the channel opens (the flip model: Burzomato *et al.* 2004). (The pre-opening conformation change was referred to as 'flipping' by them, to provide a brief way of distinguishing between this conformation change and the subsequent gating (channel-opening) conformation change.) Thirdly, more shut states than the basic nine (in Fig. 5*A*) are needed to account for the complexity of the structure of activations. Wyllie *et al.* (1998) pointed out that the long latency to the first channel opening, and the slow rise of synaptic currents, required relatively long-lived shut states, probably fully liganded, to precede opening, and that the presence of such states implied that activations would be long. Popescu & Auerbach (2003) and Banke & Traynelis (2003) made similar proposals. In the latter paper, the authors found it necessary to add two more short-lived shut states to their mechanism (Fig. 5 in Banke & Traynelis, 2003). This procedure is reminiscent of addition of extra shut states in the case of the nicotinic acetylcholine receptor, as one (again not unique) way to get a really good fit of shut-time distributions (Salamone *et al.* 1999; Hatton *et al.* 2003). However, all the variants postulated by Banke & Traynelis (2003), still contain only one open state. Therefore they can account neither for our two-component open-time distributions, nor for the appearance of correlations between open and shut times (Fig. 3*C*).

Our evidence suggests that we need at least two open states, and, to account for correlations in Fig. 3*C*, they must arise from two different shut states. Like Banke & Traynelis (2003), we found also that at least one extra shut state was needed. We tried seven variants of the mechanism shown in Fig. 5*D*, with up to three open states, and three extra short-lived shut states. Such states are sometimes referred to as brief 'desensitised' states, but with lifetimes of the order of 1 ms, they clearly are not what underlies macroscopic desensitization. They are essentially arbitrary extra shut states that are needed to fit the data, but which have no clear structural significance. The most parsimonious mechanism that gave reasonable fits is that shown in full in Fig. 5*E*. This mechanism postulates that the main (longest) open state, at the right-hand end, can occur only after both NR1 and NR2 dimers have flipped conformation. A shorter-lived open state is postulated to arise when only one subunit has flipped (in Fig. 5*E*, this is drawn as though it occurs when NR2 only has flipped, but this is arbitrary, there being no way to distinguish between the two possibilities). Likewise, it is equally arbitrary to show the single additional shut ('desensitised') state as arising from the state in which only NR1 has flipped; it could equally arise when NR2 has flipped. This model was able to describe the full range of the observed apparent shut times, and was consequently used to evaluate different recording conditions (pH, EDTA) as well as different agonist concentrations.

The mechanism shown in Fig. 5*D*, which has no 'extra' shut state, proved inadequate. This is shown in Fig. 6*A*. The distribution of apparent shut times that is predicted by HJCFIT is seen to be a very poor prediction of the observations. The fast component of shut times is missed altogether. Even when the fit was repeated with the main opening rate (β_1) fixed at 35 000 s^{-1}, to force a reasonable fit to the fast component, the result was quite unsatisfactory, as shown in Fig. 6*B*. The addition of a single short-lived shut state from one of the two 'half-flipped' states, as shown in Fig. 5*E*, dramatically improved the fit of the shut-time distribution (Fig. 7*B*), even when several patches with different agonist concentrations were fitted simultaneously. In addition the model in Fig. 5*E* was able to predict that short shut times tend to be adjacent to long open periods (Fig. 7*C*).

An example is shown in Fig. 7 of one the best fits we could get with the mechanism in Fig. 5*E*. Idealized recordings made at all four concentration combinations (solutions 1–4 in Table 1) were fitted simultaneously (with the constraints mentioned below). In previous work (e.g. Hatton *et al.* 2003) we fitted several sets of data, each set containing one record at each of several concentrations. This approach allowed us to specify errors that are estimated empirically from the scatter of the values of each rate constant between one fit and another. In this case, we decided that the amount of information that is available in each record, compared with the number of parameters to be estimated, was such that it was preferable to do one fit that contained most of the patches that we accepted

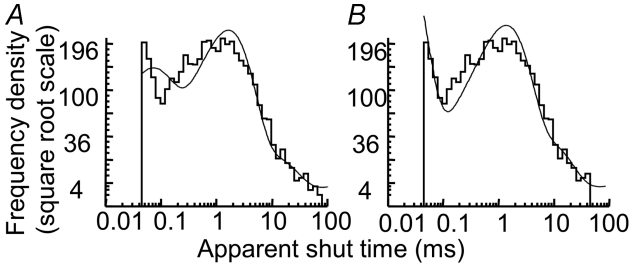

Figure 6. Representative fit using the scheme from Fig. 5*D* with the additional open state

A, HJCFIT was used to fit the mechanism in Fig. 5*A* and *D* to data from a patch recorded with low [gly] (0.85 mM [Ca^{2+}], pH 7.4). This mechanism has two open states and β_1 was left free. The predicted shut-time distribution is a poor fit to the observations. *B*, the same data and reaction scheme but now fitted with β_1 fixed at 35 000 s^{-1}. The predicted shut-time distribution is better for the fastest component, but still poor between 0.1 and 1 ms. Similar fits were generated for other patches recorded with low [gly], low [glu] and with low [glu + gly] (solutions 1–3, see Table 1). Only patches recorded with high [glu + gly] (solution 4) were fitted adequately with this scheme.

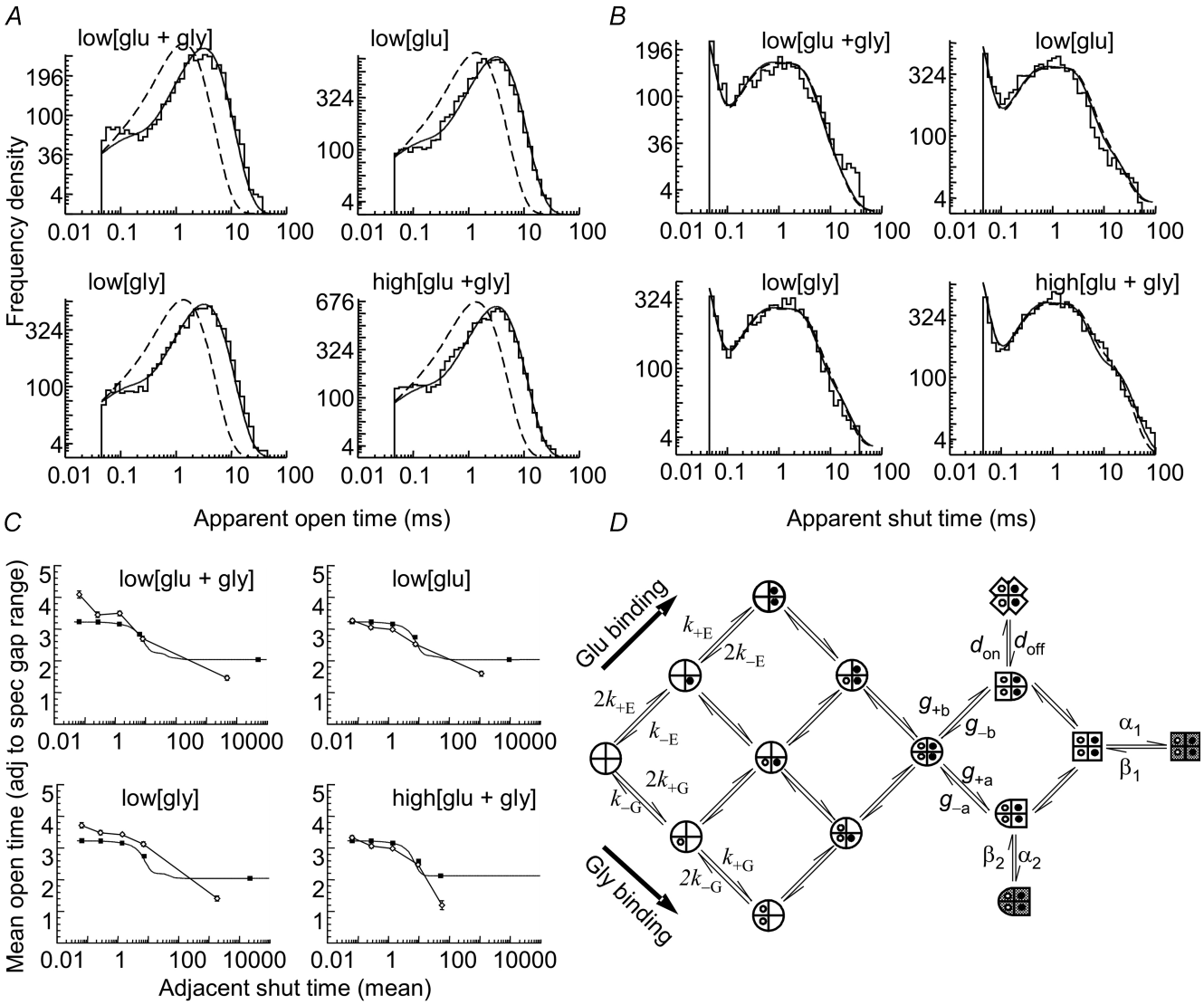

Figure 7. Simultaneous fit of data from 10 patches with the mechanism in Fig. 5*E*
Several patches from each of the four agonist conditions (low [glu + gly], 3 patches; low [glu], 2 patches; low [gly], 2 patches; high [glu + gly], 3 patches) were all fitted simultaneously with the model shown in *D* (and Fig. 5*E*). All patches where recorded in 0.85 mM $[Ca^{2+}]$ with pH 7.4 (standard $[Ca^{2+}]$ and pH; see Table 1). In *A* and *B*, the histograms are the pooled data from the patches at each concentration. The continuous curve shows the HJC distributions of *apparent* open and shut times predicted by the fit (*not* fitted to the histogram). The dashed curve shows prediction for the true distributions (perfect resolution). This figure is based on the fit with β_1 fixed at 35 000 s^{-1}, but it is not perceptibly different from the free fit, as shown by the numbers in Table 4. *A*, the predicted distribution of apparent open period. *B*, the predicted distribution of apparent shut times. *C*, prediction of correlations between open periods and adjacent shut times. The conditional mean open time plot (see Results and Fig. 3*C*). The data for the high [glu + gly] patches are plotted only up to 100 ms because these records contained few shut times longer than that. The open diamonds with error bars show the conditional mean open times from the experimental data (same data as in Fig. 3*C*). The filled squares show the HJC predictions for the apparent mean open times adjacent to shut times in the same ranges that were used for the data, calculated from the fitted rate constants in Table 4. The line that goes close to the filled squares is the continuous relationship between mean apparent open time and adjacent apparent shut time that is predicted by the fit. *D*, the reaction scheme that was fitted, with the symbols that are used for rate constants shown on the arrows. This scheme is constructed from the binding scheme shown in Fig. 5*A* and the gating scheme in Fig. 5*E*.

Table 4. Estimates of rate constants and errors from fit to 10 pooled patches with HJCFIT (see Fig. 7)

		Free fit		Fit with β_1 fixed	
Rate constant	Units	Rate	CV (%)	Rate	CV (%)
α_1	s^{-1}	734	3.5	728	0.67
β_1	s^{-1}	35 200	4.0	*35 000*	Fixed
α_2	s^{-1}	11 100	4.6	11 200	6.1
β_2	s^{-1}	788	4.3	787	6.2
d_{on}	s^{-1}	1130	3.0	1130	3.4
d_{off}	s^{-1}	925	n.d.	921	9.2
g_{-a}	s^{-1}	22 500	2.0	22 800	1.4
g_{+a}	s^{-1}	2013	3.6	2030	3.9
g_{-b}	s^{-1}	150	1.6	150	5.7
g_{+b}	s^{-1}	66.1	3.4	67.1	4.0
k_{-G}	s^{-1}	29.4	5.9	29.1	5.8
k_{+G}	$M^{-1}\ s^{-1}$	1.03×10^7	($EC_{50} = 2.6\ \mu M$)	1.0×10^7	($EC_{50} = 2.6\ \mu M$)
k_{-E}	s^{-1}	25.4	5.2	26.3	7.0
k_{+E}	$M^{-1}\ s^{-1}$	8.04×10^6	($EC_{50} = 2.9\ \mu M$)	8.3×10^6	($EC_{50} = 2.9\ \mu M$)
$E_1 = \beta_1/\alpha_1$	—	47.9	—	48.1	—
$E_2 = \beta_2/\alpha_2$	—	0.07	—	0.07	—
$G_a = g_{+a}/g_{-a}$	—	0.089	—	0.089	—
$G_b = g_{+b}/g_{-b}$	—	0.441	—	0.447	—
$D = d_{on}/d_{off}$	—	0.82	—	0.81	—
K_G	μM	2.85	—	2.91	—
K_E	μM	3.16	—	3.17	—

The results are shown for the case where β_1 was fitted freely, and for the case where β_1 was fixed at 35 000 s^{-1}.

for analysis, by the criteria given above. As in the case of nicotinic receptors (Hatton *et al.* 2003) some additional selection had to be done to eliminate patches with excess 10–20 ms shut times, or unstable amplitudes (see above). The fit shown in Fig. 7 is based on simultaneous fitting of data from 10 different patches (as specified in the legend). This method requires us to rely on the internal estimates of error provided by HJCFIT, as described, for example, by Colquhoun *et al.* (2003). It is shown in that paper that these internal estimates of error (given in Table 4) are realistic.

In Fig. 7*A* and *B*, the histograms show the distributions of the observed apparent open and shut times. The predicted (HJC) distributions of apparent open and shut times superimpose quite well on the histograms, for all four concentration combinations, and the observed open–shut correlations were predicted quite well by the fitted rate constants too (Fig. 7*C*). The rate constants found from the fit are given in Table 4, and are shown in the summary in Figs 7*D* and 10.

The amount of information in the data was not sufficient to obtain good estimates of all the rate constants in the scheme. The completely general form of Figs 5*E* and 7*D* has 38 rate constants. If we assume microscopic reversibility in the five cycles, this reduces the number of free rate constants to 33, still far too many to be defined by the data. In order to obtain reasonably well-defined values for the rate constants it proved necessary to reduced the number of free parameters to 11 or 12 (see Table 4), and this was achieved by application of the following four constraints during fitting.

Firstly it was assumed that the subunits did not interact during the binding steps, so, for example, the binding of a glutamate molecule was the same regardless of whether any other binding sites are occupied or not.

Secondly it was assumed that the flipping of the NR1 and NR2 dimers were independent, so, for example, the rate at which the NR2 dimer flips is the same regardless of whether the NR1 dimer has already flipped or not (and *vice versa*), as indicated by the labels in Fig. 5*D*.

Thirdly, the association rate constants for both glutamate and glycine were constrained so as to produce an EC_{50} for glutamate of 2.9 μM (in 30 μM glycine) and an EC_{50} for glycine of 2.6 μM (in 30 μM glutamate). These EC_{50} values were taken from previous work in the laboratory under similar conditions (Anson *et al.* 1998).

The simultaneous fit to data from 10 patches at four different concentration conditions (Fig. 7 and Table 4) allowed estimation of 12 free parameters. The results were not very sensitive to the initial guesses for the rate constants that were used for the fit. For example, if the initial guess for the main opening rate constant, β_1, was set as low as 10 000 s^{-1}, the fit still converged to about 35 000 s^{-1}. In some fits to individual concentrations, it proved difficult to get fits that described accurately the fastest shut times, and the results could be sensitive to the starting guesses, but in such cases good fits could always be obtained if β_1 was

fixed at 35 000 s^{-1}. As shown in Table 4, fixing the value of β_1 has little effect on the other estimates.

The fact that in individual experiments the free fit of β_1 sometimes produced low values, which did not fit the fast shut times well, can perhaps be taken as an indication that the constrained mechanism was not perfect. It is unlikely to result from a deficiency in the fitting method because the equivalent rate constant, the fully liganded opening rate, can be fitted as a free parameter for both nicotinic and glycine receptors, despite the fact that it is much faster than the 35 000 s^{-1} found here, especially for heteromeric glycine receptors (about 130 000 s^{-1}; Burzomato *et al.* 2004). This imperfect fit might also account for the difficulty that we encountered when trying to calculate numerically the partial second derivatives that are needed to get estimates of error when 12 free parameters were fitted, though not when β_1 was fixed. The errors for the free fits shown in Table 4 may therefore not be very accurate, but they are probably not grossly misleading. Just as in the nicotinic case (Colquhoun *et al.* 2003) there is a strong positive correlation between the estimates of α_1 and β_1 when the latter was fitted freely, but nonetheless their separate values seem to be quite well defined.

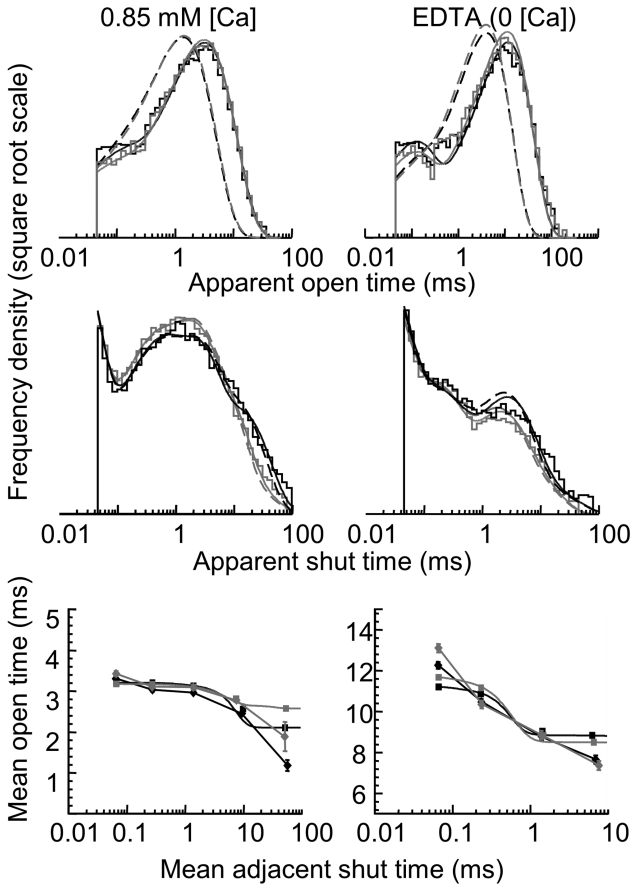

Figure 8. A fit of the mechanism in Fig. 7*D* to data from patches recorded at pH 8.0 in the presence of EDTA with saturating concentrations of both agonists

The solutions are 4–7 in Table 1. Left column: high [glu + gly]; pH 8.0, high [glu + gly]. Right column: EDTA pH 7.4, high [glu + gly], and EDTA pH 8.0, high [glu + gly]. The left column shows an overlay of patches recorded with 0.85 mm [Ca^{2+}] at pH 7.4 (black, same data as in Fig. 7, $n = 3$ patches for histogram) and pH 8.0 (grey, $n = 4$ patches, all at 100 μm glutamate and glycine). The right column shows an overlay of fits to patches recorded in the presence of 1 mm EDTA. The black data and fits are from patches recorded at pH 7.4 ($n = 3$) with 100 μm glutamate and glycine, and the grey data are from patches recorded at pH 8.0 ($n = 4$) all with 100 μm glutamate and glycine. Lines are as described for Fig. 7. The numbers of events in each histogram are as follows. Left top: black 9482 events, grey 12261. Left middle: black 9404 events, grey 12178. Right top: black 7386 events, grey 10985. Right middle: black 7305 events, grey 10985.

Fits to data at pH 8 in the presence of EDTA

Under these conditions the effects of zinc and of hydrogen ions are essentially eliminated, though only at the expense of being even further from physiological conditions than our standard (pH 7.4 with calcium) solutions. As described above (see Fig. 2), stable records, with a high P_{open} (0.88 ± 0.03) can be obtained in the presence of EDTA with saturating concentrations of glutamate and glycine. We have chosen not to concentrate our fitting efforts on such records, because the instability of patches in the absence of calcium meant that we were unable to obtain long records at low agonist concentrations.

Figure 8 shows the predictions of a fit of the same mechanism (Figs 7*D* and 10) to high concentration data alone. A reasonable, though not perfect, fit was obtained. Because of the limited amount of data, the fitted rate constants will not be given in full, but the reason for the somewhat higher P_{open} at pH 8/EDTA seemed to arise from an increase in the true mean open time of the main open state, because $1/\alpha_1$ increased from 1.4 ms (Table 4) to 3.9 ms for the fit in Fig. 8. In addition to this change in α_1 all three conditions (pH 8.0 with 0.85 [Ca^{2+}], pH 7.4 with EDTA, and pH 8.0 with EDTA) required an increase in the rates linking states 4 and 5 (as numbered in Fig. 10) and states 6 and 7. In the presence of calcium at pH 8.0 the rates increased 1.5- (state 4 to 5) and 3- (state 5 to 4) fold. In the presence of EDTA at both pH values the increases in both rates was nearly 10-fold. As in the fits for Fig. 7, we constrained the EC_{50} values for both glutamate and glycine for the fits shown in Fig. 8. In these fits, this was particularly important as all the patches used were in saturating glutamate and glycine (100 μM each) and thus contained no information about concentration dependence. In all three conditions increases in the transitions between states 6 and 7 were linked to 10-fold decreases in the dissociation rates of both glutamate and glycine. Other rates were largely unaffected by the changes in pH, but the rate of flipping from state 6 to 4 was increased 3-fold in the presence of EDTA at both pH values tested. The return rate from state 4 to 6 was decreased to 50% of that with calcium for both patches.

How well does the fit to single channel data predict macroscopic responses?

One goal of the identification of a reaction scheme is to understand the relationship between structure and function of the channel protein, and another goal is to allow prediction of the behaviour of these receptors in the synapse. As a first step toward the latter end, and as another test of the adequacy of the reaction scheme, we calculated the macroscopic response to a brief pulse of agonist using the scheme in Fig. 5*E*, with the rates shown in Table 4 and Fig. 10. The vector of state occupancies, $\boldsymbol{p}(t)$, was calculated as $\boldsymbol{p}(t) = \boldsymbol{p}(0)\exp(\boldsymbol{Q}t)$ (Colquhoun & Hawkes, 1977), with the program SCALCS. It can be seen that the current in response to a 2 ms pulse of 2 mM glutamate is predicted to rise slowly, with a sigmoid time course, and to decay slowly. The rates of rise and decay match quite well the values found in experimental concentration jump experiments that we have found previously, under very similar recording conditions (Wyllie *et al.* 1998; see Discussion).

The association rate constants for both glycine (1×10^7 M^{-1} s^{-1}) and glutamate (0.8×10^7 M^{-1} s^{-1}) are similar, and are relatively slow compared with those for acetylcholine (about 10^8 M^{-1} s^{-1}) but comparable with that for glycine binding to the resting state of the inhibitory glycine receptor (Burzomato *et al.* 2004). Nevertheless, at high agonist concentrations, as during a synaptic current, occupancy will be rapid, and the receptor becomes essentially fully liganded within 300 μs in the calculated jump response shown in Fig. 9 (which is intended to simulate a synaptic current). State 7 is reached rapidly, and all the delay in the rise of the current arises from passage from there, through states 3–6. The macroscopic relaxations are, of course, described by 14 exponential components, but in fact only one component is predominant in both the rising phase and in the decay of the macroscopic current. The largest part of the amplitude during the rising phase is an exponential with a time constant of 14.6 ms. This is remarkably close to the time constant of 13·4 ± 3·9 ms that was fitted to experimental concentrations jumps (recorded under the same conditions that we use here) by Wyllie *et al.* (1998). The decay phase in Fig. 9 is almost a pure exponential, with a time constant of 94 ms, from about 30 ms after the peak current. Wyllie *et al.* (1998) found experimentally that the decay was fitted by time constants of 71 and 350 ms.

The prediction of our fit to single channel results for the faster component of the synaptic current is quite good, but there is no slower component in our prediction. One possible reason for this is that longer-lived 'desensitised' states were omitted from our mechanism, and, although this is perfectly legitimate in the case of the nicotinic receptor (Colquhoun *et al.* 2003), it may not be for the NMDA receptor. Another possible explanation arises from the fact that our criterion for exclusion of patches based on the contribution of the 10–20 ms component of the shut-time distribution was not used in Wyllie *et al.* (1998). It is possible that inclusion of records with relatively long shut times by Wyllie *et al.* made the slow component of the decay more prominent, and also makes the predicted maximum P_{open} rather smaller that we find here.

Discussion

This paper is an attempt to fit a mechanism for both binding and gating to single channel observations on an NMDA receptor. Our model has features in common with those proposed by Banke & Traynelis (2003), Erreger *et al.* (2005) and Auerbach *et al.* (2005), but improves on them insofar as all binding steps are included, the mechanism can fit the two open states required by our data, and it can fit the observed correlation between the length of an open time and the adjacent shut time. We cannot claim that the outcome is as complete or as well-defined as has been achieved for the glycine receptor (Beato *et al.* 2002, 2004; Burzomato *et al.* 2004), or even for the nicotinic receptor (Colquhoun & Sakmann, 1985; Auerbach, 1993; Hatton *et al.* 2003). The mechanism is, *a fortiori*, unlikely to be unique. Some of the reasons for this will be discussed below.

Limitations of applicability

There are several factors that limit the applicability of these results to physiological processes. These mostly derive from various ions that can affect the behaviour of the NMDA receptor, as discussed above. Even our most physiological solutions, although they were pH 7.4 and contained calcium, lacked the magnesium that is present in real synapses, We tried, as far as possible, to minimize the zinc concentration, but the absolute concentrations in our solutions are not known either for contaminant zinc or for contaminant glycine. Another limitation of our model is that we did not aim to fit the slower forms

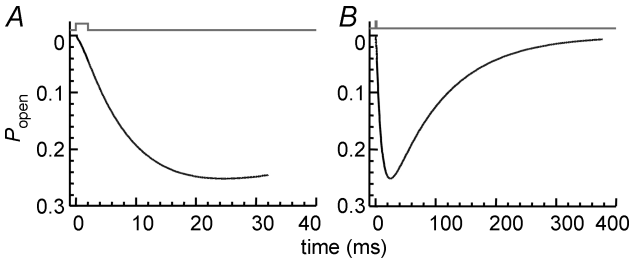

Figure 9. Prediction of the macroscopic response to a brief concentration jump, based on the fit shown in Fig. 7
The current shown is the calculated response to a 2 ms jump from 0 to 2 mM glutamate in the constant presence of 20 μM glycine (in same solution as used by Wyllie *et al*. 1998). It was calculated from the mechanism and rates shown in Fig. 10 and Table 4 (for one channel, with a membrane potential of −80 mV and a single channel conductance of 50 pS).

of desensitization, as we believe they are of marginal relevance to the physiological function of the NMDA receptor. In addition, like other groups who have modelled the behaviour of these receptors, we did not attempt to fit subconductance levels as separate states.

Limitations of the fitting

The limitations of any attempt to fit NMDA receptors are easy to state, though not easy to overcome. The difficulty lies in the combination of two facts: firstly, the individual channel activations are far more complex in structure than for a nicotinic or glycine receptor (e.g. Gibb & Colquhoun, 1992) and secondly, the lack of any detectable concentration dependence in the results reduces strongly the amount of information that we can get about the details of the mechanisms. As a result, the largest number of rate constants that we have been able to resolve is 12 (compared with up to 18 for the glycine receptor; Burzomato *et al.* 2004). The fact that there are two agonists rather than one means that the number of free rate constants in the simplest useful mechanism is 33 (assuming microscopic reversibility), so to obtain estimates it is necessary to apply four types of constraints: independence of binding sites, independence of flipping, fixing (in many cases) of one rate constant and determination of two more rates from specified EC_{50} values (more details are given in Results). We have no independent way to verify the assumptions of independence, but reasonably good fits could be obtained when they were applied, as shown in Fig. 7, so the assumptions are not grossly incompatible with our observations.

Structural implications of the mechanism

The simplest mechanism that we found that gave a good fit to single channel data in the more nearly 'physiological' conditions (pH 7.40, no Mg^{2+}, Ca^{2+} at 0.85 mM: solutions 1, 2, 3 and 4 in Table 1) has two open states and 13 shut states, including one fully liganded brief shut ('desensitised') state, as summarized in Fig. 10. It is quite complicated so it is necessary to consider the basis for the proposal.

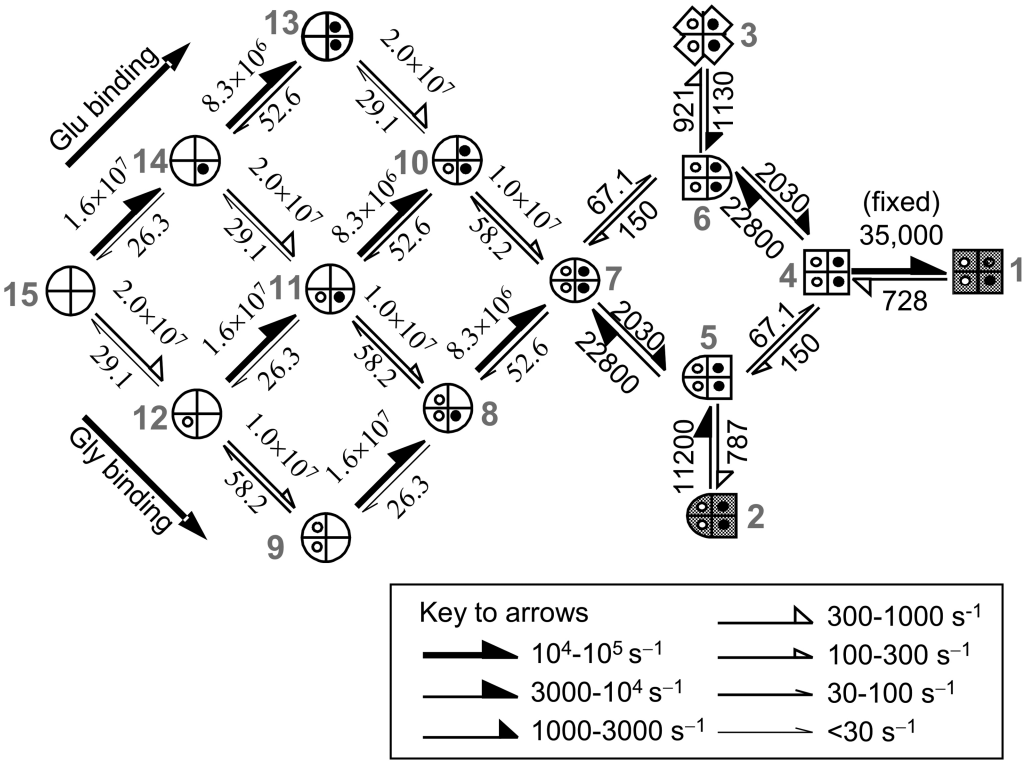

Figure 10. The reaction mechanism with the values of the rate constants that were found in the fit shown in Fig. 7

The various states of the receptor are indicated as in Fig. 5. The states are numbered from 1 to 15, to facilitate the Discussion. The arrows are labelled with the values of the rate constants that are given in Table 4, all having the dimensions of s^{-1}, except for the association rate constants (M^{-1} s^{-1}). As an additional aid to understanding the meaning of the numbers, the arrows are coded (see key, lower right) to give a visual indication of the relative speed of each transition in s^{-1}. For this purpose the association rate constant for glutamate has been multiplied by 2 mM (giving 16 600 s^{-1}), and that for glycine by 20 μM (giving 200 s^{-1}) to give the actual transition rates (in s^{-1}) that apply during the concentration jump shown in Fig. 9.

A key problem in proposing a mechanism is to decide how to connect all the shut states that are needed. It is relevant that Bruno *et al.* (2005) have proved a general result for mechanisms that show no correlations between open and shut times (for example those with only one open state, or the model 17 mechanism in Auerbach *et al.* 2005). If such mechanisms obey microscopic reversibility then *all* arrangements of shut states, for mechanisms with the same number of open and shut states, must give identical maximum likelihoods, and are therefore indistinguishable in principle, on the basis of steady-state single channel recordings at a single agonist concentration. In our case, we are slightly better off than this, because we see correlations between open and shut times, though these tell us only about the topology of the open–shut connections, not about the connections between shut states. In principle, otherwise indistinguishable mechanisms may be distinguished by fitting recordings made at different agonist concentrations. There has, so far, been no complete theoretical investigation of when this can and cannot be done, but the NMDA receptor is peculiarly bad for making this sort of distinction, because the properties of activations are, as shown here, essentially independent of the concentrations of both glutamate and glycine. The frequency of activations is, of course, dependent on concentration, but information from this source cannot be exploited because of lack of knowledge of the number of channels in the patch.

In the case of ligand-gated channels (but not voltage-gated channels), the limited ability to distinguish the nature of connections between shut states is greatly helped by structural considerations. Since a mechanism is of interest only insofar as it describes physical reality, it seems preferable, in any case, to start from structure. Given that the molecule has two binding sites for glutamate and two for glycine, the existence of the nine 'binding states' in Fig. 5*A* is inevitable. However, these states alone cannot account for the complex structure of NMDA channel activations. To do that, more shut states are needed, but their nature is largely speculative. The slow rise time of synaptic currents, and the long latency to the first channel opening after a concentration jump, require that there should be more fully liganded shut states before the channel opens. This behaviour could be mimicked as consecutive transitions through a linear sequence of shut states before the channel opens (e.g. Popescu *et al.* 2004). Such a linear sequence, although simple, does not correspond in any obvious way to physical reality and it does seem preferable to try to base the mechanism on structural considerations, albeit in a rather speculative way.

Our proposal is based on the idea that the receptor is composed of an NR1 dimer and an NR2 dimer (as suggested by Schorge & Colquhoun, 2003). We postulate that each dimer can flip to a new (still shut) conformation in a way that is independent of the state of the other dimer. Banke & Traynelis (2003) took a similar view, and our postulate is an elaboration of theirs. The main opening occurs only when both dimers have flipped. Even if this is basically correct, the limited resolving power of the observations (see above) leaves many unknowns. We need a second, brief, open state, but putting it (as in state 2 in Fig. 10) coming from a state with only one dimer flipped is arbitrary (though the existence of open–shut correlations requires some such arrangement). Likewise the origin of the extra short-lived shut ('desensitised') state (state 3 in Fig. 10) is quite arbitrary. Even if the basic layout is correct we cannot tell whether the short-lived shut state arises when the NR1–NR1 dimer has flipped, or when the NR2–NR2 dimer has flipped. Indeed, the mechanism would be formally the same if the two 'dimers' both consisted of NR1–NR2 rather than NR1–NR1 and NR2–NR2. The mechanism also makes no explicit allowance for the block by hydrogen ions that is expected at pH 7.4 (Traynelis & Cull-Candy, 1990). The effect of this block is bundled in the values of the rate constants that we find.

The results from fits at pH 8.0 and in the presence of EDTA, provide an additional hint about the structure of the receptor. All of the fits in these conditions changed the flipping rates g_{+B} and g_{-B} between states 4 and 5 (see Fig. 10), as well as those between states 6 and 7 (which were constrained to be equal to those between states 4 and 5 for independent subunits). The specificity for one set of gating rates suggests that both calcium and protons may act on the same dimer within the receptor. These results are still very preliminary, but follow-up work looking at receptors with different NR2 subunits or partial agonists may indicate whether the specificity of the changes for one set of 'flip' rates may be maintained in other receptor subunit compositions (see Erreger *et al.* 2005).

Comparisons with other recent work

Since this work was completed, two studies of the mechanisms of NMDA receptor activation have appeared (Erreger *et al.* 2005 and Auerbach *et al.* 2005). The results for macroscopic jumps given by Auerbach *et al.* (2005) are similar to those of Wyllie *et al.* (1998), though Erreger *et al.* (2005) get somewhat faster deactivation rates, perhaps because they express the receptors in HEK cells, rather than in the *Xenopus* oocytes used in the other work to which we refer.

Despite many similarities, our results differ in two important respects from theirs. Firstly, our main channel opening rate constant (β_1, Table 4) is considerably faster than was estimated by either of these authors, or by earlier studies. The review by Erreger *et al.* (2004) lists (in their Table 5) 32 different estimates of the opening rate constant. They range from 10 to 100 s^{-1} in the 1990s, and rise to about 1500–3000 s^{-1} in recent work. To these can be added

the fastest estimate so far, of over 5000 s^{-1} in Auerbach *et al.* (2005). In contrast, our results suggest a much faster value than any of these, of the order of 35 000 s^{-1}, much like a nicotinic or glycine receptor.

The other major difference between our work and others is that Auerbach *et al.* (2005) report that their data show no correlations between adjacent open and shut times, whereas we see such correlations, both here (Figs 3 and 7), and in our earlier work (e.g. Gibb *et al.* 1992). This observation leads Auerbach and Zhou to arrange their two open states in a different way from us.

It seems possible that the explanation for both of these apparent discrepancies (large β_1 and presence of correlations) lies in the same problem, namely the ability to detect the fastest component of the shut-time distribution. It is this component that is most important in determination of the opening rate constant, and its detection is important for assessment of correlations. We find (Table 2) the fastest component of the shut-time distribution has a time constant of about 20 μs (with roughly 50% of the area), somewhat faster than the value of 45 μs found by Wyllie *et al.* (1998), but much faster than the value of 140–170 μs found in Auerbach *et al.* (2005). Erreger *et al.* (2005) mention a fast component of around 100 μs but do not resolve it clearly. One possible explanation for this discrepancy lies in the analysis methods. The resolution was set conservatively to 45 μs in this work, but it was 100 μs in Erreger *et al.* (2005), in part, at least, because outside-out patches from HEK cells are noisier than those from oocytes. Auerbach *et al.* (2005) fitted their data with a resolution of '2–3 sampling intervals (50–75 μs)'. Resolution is important because the ability to resolve this fast shut time seems to be critical for detecting correlations between the open and shut states. Auerbach *et al.* (2005) measure correlations between open and shut times as autocorrelations (expressed as a function of lag), rather than as the conditional mean open times which we prefer to use to provide a synoptic view of such correlations. Figure 11*A* shows open–shut autocorrelations found from our data, recorded under similar conditions to theirs (outside-out patches from oocytes in the presence of EDTA (solution 7, EDTA 8.0, high [glu + gly], Table 1), and expressed in the same way as Auerbach *et al.* (2005, their Fig. 2). With our usual resolution of 45 μs, there is a clear negative correlation between open time and the following shut time (lag = 1) though it is not detectable for great lags. However, if we impose a resolution of 100 μs on the same data, many of the shortest shuttings are removed, and the correlations become undetectable, as shown in Fig. 11*B*. These autocorrelation plots (like those of Auerbach *et al.* 2005) are not corrected for missed events (whereas the conditional mean

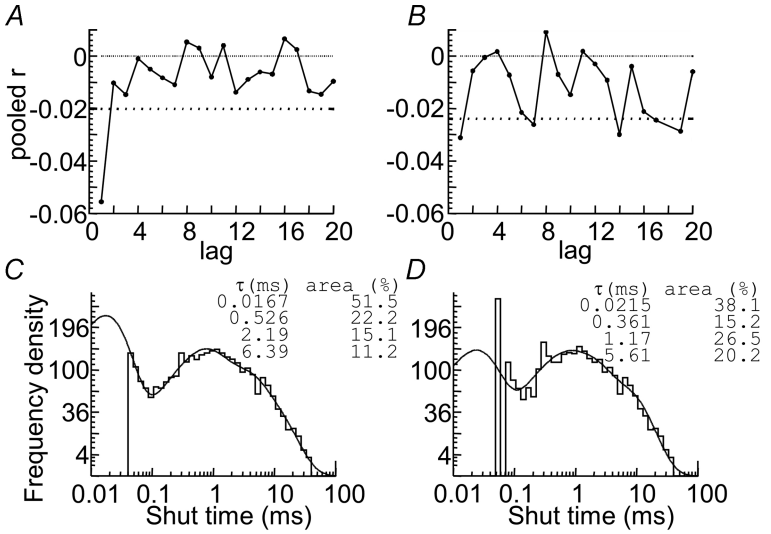

Figure 11. Effects of lowering resolution, and of rounding dwell times
A and *B* show the autocorrelation between apparent open and shut times as a function of lag (lag = 1 for open time and adjacent shut time, lag = 2 for open time and the next but one shut time, etc.; see Colquhoun & Hawkes, 1987). Data recorded in pH 8 + EDTA (solution 7, Table 1), as in Figs 2 and 8 (right column). *A*, for adjacent open and shut times (lag = 1) the correlation is negative and clearly outside the dashed line that shows approximately two standard deviations below zero (resolution 45 μs). *B*, when an artificially low resolution of 100 μs is imposed on the same data, the correlation becomes undetectable. These plots (like those of Auerbach *et al*. 2005) are not corrected for missed events. *C* and *D* show histograms of shut times, recorded as in Figs 1 and 7 (high [glu + gly], solution 4, Table 1). In *C* the empirical fit of four exponential components is shown. In *D*, the same data have been rounded to integer multiples of 25 μs, and fitted in the same way. The loss of information caused by rounding is obvious.

method of displaying correlations shown in Figs 7 and 8, uses HJC distributions which employ exact correction for missed events).

As well as problems of resolution, it may be equally important that both Erreger *et al.* (2005) and Auerbach *et al.* (2005) idealize their data using the SKM method, which does not give durations of dwell times on a continuous time scale, but as integer multiples of the sampling interval. Thus, for example, in Fig. 4 of Erreger *et al.* (2005), the shut times would be restricted to values of 100 μs, 125 μs, 150 μs, etc., rather than being on a continuous scale. This rounding does not matter much for long intervals, but it must inevitably lead to loss of valuable information about the fastest component (which, at 20 μs in our data is less than the smallest multiple of the sampling interval of 25 μs). In order to test the possible importance of this, we looked at the effect of artificially rounding all shut times to the nearest 25 μs, after a resolution of 40 μs had been imposed on them. The histogram in Fig. 11*C* shows our original shut-time distribution for a patch recorded in our standard conditions (solution 4, high [glu + gly], Table 1), and the histogram in Fig. 11*D* shows the same data after rounding the intervals. Notice that the first and third bins are completely empty in Fig. 11*D*. This itself may not matter, because the fitting of exponentials does not use the bin frequencies, but when both distributions are fitted with a mixture of four exponential probability density functions, it is seen that the rounding causes the time constant to be overestimated and the area of the fastest shut-time component to be underestimated quite seriously. A qualitatively similar effect was found with data recorded in EDTA (solution 7, EDTA 8.0, high [glu + gly], Table 1). The effect of rounding on the fitting of mechanisms (as opposed to exponentials) has not been investigated, but the fits obtained by the QUB program do not seem to fit at all the short shut times in their data (Erreger *et al.* 2005, their Fig. 4). We conclude that methods, like SKM, which discard information about the distribution of the important short shut times, may result in sufficiently large changes in the fitting of short intervals that the interpretation of the data is altered. Some threshold crossing methods of analysis also round dwell times in this way, though others do not.

Interpretation of the results

If we take at face value the mechanism (Fig. 10) and the values of the rate constants (Table 4, Fig. 7*D*), it is interesting to see how they explain both single channel and macroscopic behaviour. Figure 10 gives a simpler view of the rate of each reaction step by encoding the rate in the style of the arrows.

At the bottom of Table 4, we give some of the equilibrium constants, calculated from the estimated rate constants. It is seen that the main gating constant ('efficacy') is actually quite high ($E_1 = 48.1$, much the same as for a nicotinic or glycine receptor). The gating constant for the brief open state, which carries little current, is much lower ($E_2 = 0.07$). The maximum response is limited not by the main gating constant, which is high, but by the pre-opening conformation changes (states 4, 5, 6 and 7).

It will be helpful to make a comparison with the simpler case of the inhibitory glycine receptor. The 'flip' model describes the fully liganded receptor thus:

$$A_3R \underset{F_3}{\rightleftharpoons} A_3F \underset{E_3}{\rightleftharpoons} A_3F^*$$

where A represents the agonist. The resting conformation (R) changes conformation to a 'flipped' conformation (F) while still shut, and from the flipped conformation it can then change conformation again to the open state (F*). The equilibrium constant (F_3) for flipping is 27 and the main gating constant (E_3) is 20 (Burzomato *et al.* 2004). The fraction in the open state, the maximum P_{open}, is $F_3E_3/(1 + F_3 + F_3E_3) = 0.95$ for the glycine receptor (Burzomato *et al.* 2004).

The fully liganded NMDA receptor is a bit more complicated. The rate constant estimates in Fig. 10 imply that the maximum P_{open} with both agonists saturating, for the receptor (solution 4, high [glu + gly], Table 1) is close to 0.5, consistent with our data. Thus, despite the high value for the main gating constant ($E_1 = 48$), the agonists, jointly, seem to work as partial agonists, because the pre-opening conformation changes in the saturated states (4, 5, 6 and 7 in Fig. 10) limit the maximum response. The flipping constant, F_3, for the glycine receptors example is replaced by the overall equilibrium constant for saturated pre-opening conformation changes (the ratio of state 4 to state 7 at equilibrium) and is $G_aG_b = 0.0397$, which is very low, compared with the gating constant of 48 (the corresponding values for the glycine receptor are 27 and 20, respectively). If we neglect the D state and the minor open state, the maximum P_{open} for Fig. 10 would be $G_aG_bE_1/(1 + G_aG_b + G_aG_bE_1)$, and since $G_aG_b \ll 1$, the effective overall efficacy is approximately $G_a\ G_b\ E_1 = 1.9$, which implies a maximum P_{open} of 0.65. However, the existence of the D state reduces the exact maximum P_{open} to 0.5 for the values in Fig. 10.

It seems likely that limitation on overall efficacy that results from the low (0.0397) equilibrium constant for the pre-opening conformation changes is largely a consequence of proton block of the receptor at pH 7.4, and we have not explicitly included the proton block in the mechanism because of uncertainty about how it works. Similar remarks apply to the effects of calcium and zinc which may also contribute to the appearance of partial agonism. When proton and divalent ion concentrations are minimized, at pH 8, with EDTA (see Table 1), the fitted rate constants imply a maximum P_{open} of 0.905, almost as

high as for nicotinic and glycine receptors, and close to the observed value of 0.88 ± 0.03.

The numbers shown in Fig. 10 suggest the following steps are likely to occur (see state numbering in Fig. 10, grey). At low agonist concentration binding will not be rapid, but at equilibrium, once the fully liganded state 7 is reached the rates for flipping are large compared with the rather slow dissociation rates for both glutamate and glycine. This means that flipping (largely to state 5) is quite likely once state 7 has been reached, and this may lead to opening. After an opening to state 1, the main open state, the channel must return to the adjacent shut state (4) from where it is likely to re-open a few times after very short shuttings (the mean lifetime of state 4 is 17 μs). If the channel does not re-open it is most likely to return to state 6, from which return to state 4 (and possible re-opening) is more likely than return to state 7, thus generating longer shut times within the fully liganded activation. Finally, when the channel does get back to state 7, it is again more likely to flip than dissociate, and so may again re-open, but after a still longer shut time. All these oscillations between states occur while the channel is still fully liganded. The complex distribution of shut times within an activation can therefore arise because after an opening the channel may re-open immediately, but may also 'go back' one or two steps before re-opening.

Our fitting was entirely to records of single channel currents in the steady state, but once we have the mechanism in Fig. 10 and the rates in Table 4, it is easy to calculate the time course of receptor occupancy during a concentration jump, by standard eigenvalue methods (Colquhoun & Hawkes, 1977). Considering that these predictions were made entirely from single channel results, their agreement with observation, if not quite as perfect as for the glycine receptor (Burzomato *et al.* 2004), is quite impressive and lends strength to the general form of our proposed mechanism.

References

Anson LC, Chen PE, Wyllie DJ, Colquhoun D & Schoepfer R (1998). Identification of amino acid residues of the NR2A subunit that control glutamate potency in recombinant NR1/NR2A NMDA receptors. *J Neurosci* **18**, 581–589.

Ascher P & Nowak L (1988). The role of divalent cations in the *N*-methyl-D-aspartate responses of mouse central neurones in culture. *J Physiol* **399**, 247–266.

Auerbach A (1993). A statistical analysis of acetylcholine receptor activation in *Xenopus* myocytes: stepwise *versus* concerted models of gating. *J Physiol* **461**, 339–378.

Auerbach A & Zhou Y (2005). Gating reaction mechanisms for NMDA receptor-channels. *J Neurosci* **25**, 7914–7923.

Banke TG, Dravid SM & Traynelis SF (2005). Protons trap NR1/NR2B NMDA receptors in a nonconducting state. *J Neurosci* **25**, 42–51.

Banke TG & Traynelis SF (2003). Activation of NR1/NR2B NMDA receptors. *Nat Neurosci* **6**, 144–152.

Beato M, Groot-Kormelink PJ, Colquhoun D & Sivilotti LG (2002). Openings of the rat recombinant alpha 1 homomeric glycine receptor as a function of the number of agonist molecules bound. *J General Physiol* **119**, 443–466.

Beato M, Groot-Kormelink PJ, Colquhoun D & Sivilotti LG (2004). The activation mechanism of alpha1 homomeric glycine receptors. *J Neurosci* **24**, 895–906.

Béhé P, Stern P, Wyllie DJ, Nassar M, Schoepfer R & Colquhoun D (1995). Determination of NMDA NR1 subunit copy number in recombinant NMDA receptors. *Proc Biol Sci* **262**, 205–213.

Benveniste M & Mayer ML (1991). Kinetic analysis of antagonist action at N-methyl-D-aspartic acid receptors. Two binding sites each for glutamate and glycine. *Biophys J* **59**, 560–573.

Blatz AL & Magleby KL (1989). Adjacent interval analysis distinguishes among gating mechanisms for the fast chloride channel from rat skeletal muscle. *J Physiol* **410**, 561–585.

Bruno WJ, Yang J & Pearson JE (2005). Using independent open-to-closed transitions to simplify aggregated Markov models of ion channel gating kinetics. *Proc Natl Acad Sci U S A* **102**, 6326–6331.

Burzomato V, Beato M, Groot-Kormelink PJ, Colquhoun D & Sivilotti LG (2004). Single-channel behavior of heteromeric alpha1beta glycine receptors: an attempt to detect a conformational change before the channel opens. *J Neurosci* **24**, 10924–10940.

Clements JD & Westbrook GL (1991). Activation kinetics reveal the number of glutamate and glycine binding sites on the N-methyl-D-aspartate receptor. *Neuron* **7**, 605–613.

Colquhoun D, Hatton CJ & Hawkes AG (2003). The quality of maximum likelihood estimates of ion channel rate constants. *J Physiol* **547**, 699–728.

Colquhoun D & Hawkes AG (1977). Relaxation and fluctuations of membrane currents that flow through drug-operated channels. *Proc Roy Soc Lond B* **199**, 231–262.

Colquhoun D & Hawkes AG (1982). On the stochastic properties of bursts of single ion channel openings and of clusters of bursts. *Phi Trans Roy Soc Lond B* **300**, 1–59.

Colquhoun D & Hawkes AG (1987). A note on correlations in single ion channel records. *Proc R Soc Lond B Biol Sci* **230**, 15–52.

Colquhoun D & Hawkes AG (1995). The principles of the stochastic interpretation of ion-channel mechanisms. In *Single-Channel Recording*, ed. Sakmann B & Neher E, pp. 397–482. Plenum Press, New York.

Colquhoun D, Hawkes AG, Merlushkin A & Edmonds B (1997). Properties of single ion channel currents elicited by a pulse of agonist concentration or voltage. *Philos Trans R Soc Lond A* **355**, 1743–1786.

Colquhoun D, Hawkes AG & Srodzinski K (1996). Joint distributions of apparent open and shut times of single-ion channels and maximum likelihood fitting of mechanisms. *Philos Trans R Soc Lond A* **354**, 2555–2590.

Colquhoun D & Sakmann B (1981). Fluctuations in the microsecond time range of the current through single acetylcholine receptor ion channels. *Nature* **294**, 464–466.

Colquhoun D & Sakmann B (1985). Fast events in single-channel currents activated by acetylcholine and its analogues at the frog muscle end-plate. *J Physiol* **369**, 501–557.

Colquhoun D & Sigworth F (1995). Fitting and statistical analysis of single-channel records-channel mechanisms. In *Single-Channel Recording*, ed. Sakmann B & Neher E, pp. 483–587. Plenum Press, New York.

Cull-Candy S, Brickley S & Farrant M (2001). NMDA receptor subunits: diversity, development and disease. *Curr Opin Neurobiol* **11**, 327–335.

Dingledine R, Borges K, Bowie D & Traynelis SF (1999). The glutamate receptor ion channels. *Pharmacol Rev* **51**, 7–61.

Edmonds B, Gibb AJ & Colquhoun D (1995). Mechanisms of activation of muscle nicotinic acetylcholine receptors and the time course of endplate currents. *Annu Rev Physiol* **57**, 469–493.

Erreger K (2002). Zinc and protons similarly modulate single-channel kinetics of NMDA receptors. *Soc Neuroscience Abstract* 639.2.

Erreger K, Chen PE, Wyllie DJ & Traynelis SF (2004). Glutamate receptor gating. *Crit Rev Neurobiol* **16**, 187–224.

Erreger K, Dravid SM, Banke TG, Wyllie DJ & Traynelis SF (2005). Subunit-specific gating controls rat NR1/NR2A and NR1/NR2B NMDA channel kinetics and synaptic signalling profiles. *J Physiol* **563**, 345–358.

Fredkin DR, Montal M & Rice JA (1985). Identification of aggregated Markovian models: application to the nicotinic acetylcholine receptor. In *Proceedings of the Berkeley Conference in Honor of Jerzy Neyman and Jack Kiefer*, ed.Le Cam LM, pp. 269–289. Monterey, Wadsworth.

Gibb AJ & Colquhoun D (1992). Activation of *N*-methyl-D-aspartate receptors by L-glutamate in cells dissociated from adult rat hippocampus. *J Physiol* **456**, 143–179.

Gibb AJ & Edwards FA (1991). Glycine does not alter the properties of single clusters of NMDA channel openings in outside-out patches from rat hippocampal granule cells. *J Physiol* **438**, 254P.

Hatton CJ & Paoletti P (2005). Modulation of triheteromeric NMDA receptors by N-terminal domain ligands. *Neuron* **46**, 261–274.

Hatton CJ, Shelley C, Brydson M, Beeson D & Colquhoun D (2003). Properties of the human muscle nicotinic receptor, and of the slow-channel myasthenic syndrome mutant εL221F, inferred from maximum likelihood fits. *J Physiol* **547**, 729–760.

Hawkes AG, Jalali A & Colquhoun D (1990). The distributions of the apparent open times and shut times in a single channel record when brief events can not be detected. *Philos Trans R Soc Lond A* **332**, 511–538.

Hawkes AG, Jalali A & Colquhoun D (1992). Asymptotic distributions of apparent open times and shut times in a single channel record allowing for the omission of brief events. *Philos Trans R Soc Lond B Biol Sci* **337**, 383–404.

Husi H, Ward MA, Choudhary JS, Blackstock WP & Grant SG (2000). Proteomic analysis of NMDA receptor-adhesion protein signaling complexes. *Nat Neurosci* **3**, 661–669.

Jalali A & Hawkes AG (1992*a*). The distribution of apparent occupancy times in a two-state Markov process in which brief events can not be detected. *Adv Appl Probability* **24**, 288–301.

Jalali A & Hawkes AG (1992*b*). Generalised eigenproblems arising in aggregated Markov processes allowing for time interval omission. *Adv Appl Probability* **24**, 302–321.

Johnson JW & Ascher P (1987). Glycine potentiates the NMDA response in cultured mouse brain neurons. *Nature* **325**, 529–531.

Johnson JW & Ascher P (1990). Voltage-dependent block by intracellular Mg^{2+} of N-methyl-D-aspartate-activated channels. *Biophys J* **57**, 1085–1090.

Kleckner NW & Dingledine R (1988). Requirement for glycine in activation of NMDA-receptors expressed in Xenopus oocytes. *Science* **241**, 835–837.

Lester RA & Jahr CE (1992). NMDA channel behavior depends on agonist affinity. *J Neurosci* **12**, 635–643.

Lester RA, Tong G & Jahr CE (1993). Interactions between the glycine and glutamate binding sites of the NMDA receptor. *J Neurosci* **13**, 1088–1096.

Low CM, Zheng F, Lyuboslavsky P & Traynelis SF (2000). Molecular determinants of coordinated proton and zinc inhibition of N-methyl-D-aspartate NR1/NR2A receptors. *Proc Natl Acad Sci U S A* **97**, 11062–11067.

Nahum-Levy R, Lipinski D, Shavit S & Benveniste M (2001). Desensitization of NMDA receptor channels is modulated by glutamate agonists. *Biophys J* **80**, 2152–2166.

Paoletti P, Ascher P & Neyton J (1997). High-affinity zinc inhibition of NMDA NR1-NR2A receptors. *J Neurosci* **17**, 5711–5725.

Popescu G & Auerbach A (2003). Modal gating of NMDA receptors and the shape of their synaptic response. *Nat Neurosci* **6**, 476–483.

Popescu G, Robert A, Howe JR & Auerbach A (2004). Reaction mechanism determines NMDA receptor response to repetitive stimulation. *Nature* **430**, 790–793.

Rycroft BK & Gibb AJ (2004). Regulation of single NMDA receptor channel activity by alpha-actinin and calmodulin in rat hippocampal granule cells. *J Physiol* **557**, 795–808.

Salamone FN, Zhou M & Auerbach A (1999). A re-examination of adult mouse nicotinic acetylcholine receptor channel activation kinetics. *J Physiol* **516**, 315–330.

Schorge S & Colquhoun D (2003). Studies of NMDA receptor function and stoichiometry with truncated and tandem subunits. *J Neurosci* **23**, 1151–1158.

Stern P, Behe P, Schoepfer R & Colquhoun D (1992). Single-channel conductances of NMDA receptors expressed from cloned cDNAs: comparison with native receptors. *Proc Biol Sci* **250**, 271–277.

Traynelis SF & Cull-Candy SG (1990). Proton inhibition of N-methyl-D-aspartate receptors in cerebellar neurons. *Nature* **345**, 347–350.

Twyman RE & Macdonald RL (1991). Kinetic properties of the glycine receptor main- and sub-conductance states of mouse spinal cord neurones in culture. *J Physiol* **435**, 303–331.

Wyllie DJ, Behe P & Colquhoun D (1998). Single-channel activations and concentration jumps: comparison of recombinant NR1a/NR2A and NR1a/NR2D NMDA receptors. *J Physiol* **510**, 1–18.

Wyllie DJ, Behe P, Nassar M, Schoepfer R & Colquhoun D (1996). Single-channel currents from recombinant NMDA NR1a/NR2D receptors expressed in Xenopus oocytes. *Proc Biol Sci* **263**, 1079–1086.

Acknowledgements

We would like to thank Hélène Castel and Philippe Béhé for many valuable discussions during the course of this work, David Wyllie for careful reading and discussion of the manuscript, and Dimitri Kullmann for generous support and encouragement. This work was supported by the Medical Research Council and the Wellcome Trust.

Authors' present addresses

S. Schorge: Department of Clinical and Experimental Epilepsy, Institute of Neurology, UCL, Queen Square, London WC1N 3BG, UK.

S. Elenes: University Center For Biomedical Research, University of Colima, Colima, Mexico.